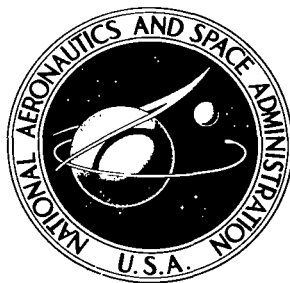


NASA TECHNICAL NOTE



NASA TN D-5018

C.1

NASA TN D-5018

0131693



TECH LIBRARY KAFB, NM

LOAN COPY: RETURN TO  
AFWL (WLIL-2)  
KIRTLAND AFB, N MEX

SUPERSONIC TRANSPORT OPERATING  
PRACTICES DURING SIMULATED OPERATIONS  
IN FUTURE AIR TRAFFIC  
CONTROL SYSTEM ENVIRONMENTS

*by Milton D. McLaughlin and Richard H. Sawyer*

*Langley Research Center*

*Langley Station, Hampton, Va.*



0131693

NASA TN D-5018

SUPERSONIC TRANSPORT OPERATING PRACTICES DURING  
SIMULATED OPERATIONS IN FUTURE AIR TRAFFIC  
CONTROL SYSTEM ENVIRONMENTS

By Milton D. McLaughlin and Richard H. Sawyer

Langley Research Center  
Langley Station, Hampton, Va.

NATIONAL AERONAUTICS AND SPACE ADMINISTRATION

---

For sale by the Clearinghouse for Federal Scientific and Technical Information  
Springfield, Virginia 22151 - CFSTI price \$3.00

**SUPERSONIC TRANSPORT OPERATING PRACTICES DURING  
SIMULATED OPERATIONS IN FUTURE AIR TRAFFIC  
CONTROL SYSTEM ENVIRONMENTS**

By Milton D. McLaughlin and Richard H. Sawyer  
Langley Research Center

**SUMMARY**

Operating practices of the supersonic transport (SST) during simulated operations in air traffic control (ATC) system environments conceived for the time period for introduction of the SST into service are presented. An SST flight simulator and the Federal Aviation Administration ATC simulation facilities were used to create the real-time simulations. The SST flight simulator was operated by airline crews and the ATC simulation facilities by experienced air traffic controllers. The test program included departure and arrival operations under instrument flight rule conditions in the New York and Los Angeles terminal areas with two design study configurations of the SST. The design study configurations were representative of variable-sweep and fixed-wing designs. Both designs had a variable-incidence forebody.

The investigation showed that the forebody placard speed was exceeded with the forebody deflected on a number of occasions in both climbs and descents with both SST configurations; thus, there is a need for an aural overspeed warning in addition to the overspeed warning light. The pilots commented that the forebody placard speed should be high enough to allow the forebody to be fully deflected for all subsonic-speed operations. For the variable-sweep-wing SST configuration, flaps and spoilers were often used at subsonic speeds in descents because of the low slowup and descent-angle capability of the clean configuration. The flap placard speed was exceeded on occasion when the flap was deflected to the landing configuration for these purposes. For the fixed-wing SST (not equipped with flaps or spoilers), the landing gear was often extended as a drag-increasing device for slowup or to steepen the descent; use of the landing gear for these purposes resulted in a number of incidents in which the landing-gear placard speed was exceeded. The crew failed to comply with the wing-sweep schedule on many occasions; therefore, a need for a wing-sweep warning device is indicated. For portions of the climbs and descents in which the scheduled speed was close to or equal to the maximum operating limit speed, many overspeed events occurred during manually controlled flight. In 9 hours of manually controlled cruising flight under calm-air standard atmospheric conditions,

111 overspeed incidents were noted; the maximum overspeed Mach number increment measured was 0.05. In cruise flight, pilots were forced to monitor the speed almost continuously and to make throttle adjustments on the order of one every 3 to 5 minutes.

## INTRODUCTION

Tentative airworthiness standards for the supersonic transport (SST) have been developed by the Federal Aviation Administration (FAA) to serve as guidelines during the design and development phases of this aircraft (ref. 1). In general, these tentative standards have been based on subsonic jet transport operational experience, military and research operational experience with high performance supersonic aircraft, and analytical and simulation studies. Development of these standards has been hampered by lack of commercial operational experience with aircraft similar to the SST. In particular, knowledge is lacking on SST operating practices as determined by the combined effects of aircraft performance, airline operating procedures, and the air traffic environment.

In order to provide additional information pertinent to the development of SST airworthiness standards, an analysis was made of SST operating practices which occurred during a cooperative NASA-FAA simulation program of the SST in the air traffic control (ATC) systems. This SST-ATC program was basically designed to study the problems connected with the introduction of the SST into the ATC system. The program included real-time simulation of two design study configurations of the SST in air-traffic-control environments representing present-day and future conditions in such terminal areas as New York and Los Angeles. The design study configurations were representative of variable-sweep and fixed-wing designs. Both designs had a variable-incidence forebody. Airline crews flew the SST airplane flight simulator and experienced air traffic controllers manned the ATC facilities. The primary results from this program have been reported in references 2 to 6. The operating-practice results obtained from this program and presented in this paper include climb and descent performance, operating speed practices, and overspeed events. These results are limited to the studies made in the ATC environments conceived for the 1970-1975 time period.

## SYMBOLS

D	drag, pounds force (newtons)
$\dot{h}$	vertical speed, feet/minute (meters/minute)
M	Mach number

$M_{MO}$	maximum operating limit Mach number
$\Delta p$	sonic-boom overpressure level, pounds force/square foot (newtons/meter <sup>2</sup> )
$T$	thrust, pounds force (newtons)
$(T/W)_{TO}$	thrust-weight ratio at take-off
$V_D$	design dive speed, knots
$V_{MO}$	maximum operating limit speed, knots
$V_R$	rotation speed, knots
$V_1$	critical-engine-failure speed, knots
$V_2$	take-off safety speed, knots
$W$	weight, pounds force (newtons)
$\gamma$	flight-path angle, degrees
$\theta$	pitch attitude, degrees
$\Lambda$	sweepback angle, degrees

#### NOTATIONS

ATC	air traffic control
DME	distance measuring equipment
FAA	Federal Aviation Administration
FL	flight level
IFR	instrument flight rules
ILS	instrument landing system

<b>JFK</b>	John F. Kennedy International Airport
<b>KIAS</b>	indicated airspeed, knots
<b>LAX</b>	Los Angeles International Airport
<b>NAFEC</b>	National Aviation Facilities Experimental Center (FAA)
<b>NASA</b>	National Aeronautics and Space Administration
<b>SID</b>	standard instrument departure
<b>SST</b>	supersonic transport
<b>VHF</b>	very high frequency
<b>VOR</b>	VHF omni-range radio navigation station
<b>VORTAC</b>	VOR station with DME provision

## EQUIPMENT

A block diagram of the NASA and FAA facilities used in this study and the interconnections of this equipment are given in figure 1. At the NASA Langley Research Center, an aircraft flight simulator linked to the analog computer facility was used to represent the SST design being investigated. This equipment was connected to the FAA air traffic control (ATC) simulator at the National Aviation Facility Experimental Center (NAFEC) in Atlantic City, New Jersey, by means of data and voice lines.

### SST Simulator

The flight compartment of the fixed-base aircraft flight simulator used to represent the SST was similar to that of current jet transport aircraft. (See fig. 2.) The basic flight instrumentation included displays having various combinations of drum, counter, and pointer indicators, a moving tape display, a vertical-scale moving pointer display, and a modern flight director system. The controls and displays pertinent to operating practices are labeled. The SST simulator included accessory equipment for navigation, communication (including an ATC beacon transponder), and data transmission. The radio-aids equipment provided simulation of VORTAC stations, marker beacons, and ILS stations. The

communications equipment simulated VHF radio communications between the pilots and air traffic controllers over the telephone lines.

The characteristics of the SST under study were programed on five dc analog computers. Six-degree-of-freedom equations were used in the representation of the airplane motions. The characteristics of the engines and other airplane systems were also programed in the computers.

Characteristics of airplane designs used in SST simulator.- Two U.S. design study configurations were used in the SST simulator. Each was designed to have a cruise Mach number of 2.7. Configuration A employed a variable-sweep wing and configuration B employed a double-delta wing. Both configurations were equipped with thrust augmentators. For each configuration, the international and domestic versions were based on the same airframe. For configuration A, the same engines were used on both versions; however, for configuration B, the engines were scaled down in the lighter domestic version to retain the same take-off thrust-weight ratio as the international version. (See table I.) The minimum transonic acceleration values given in table I are for operations restricted by a sonic-boom overpressure limit of 2.0 lbf/ft<sup>2</sup> (95.7 N/m<sup>2</sup>) for the domestic versions, 2.5 lbf/ft<sup>2</sup> (119.7 N/m<sup>2</sup>) for the international version of configuration B, and unrestricted overpressure limit ( $V_{MO}$  climbout) for the international version of configuration A. The wing-loading values are for the take-off condition.

For both configurations, the basic airplane damping was augmented about all three axes so that the results would not be affected by the handling qualities. In addition to a variable-sweep wing, configuration A was equipped with a retractable landing gear, a two-position forebody, flaps, and spoilers. Configuration B was equipped only with a retractable landing gear and a three-position forebody. The indicators, warning lights, and controls used in operating and monitoring these systems are shown in figure 2. The operating and monitoring equipment used with these systems is presented in table II. Placard speeds (structural-design operational-speed limitations) connected with these systems are presented in table III and were posted in the cockpit for use by the flight crews. An aural overspeed warning device was programed to sound at 6 KIAS above  $V_{MO}$  simultaneously with the illumination of the red overspeed warning light.

#### Air Traffic Control Simulator

The real-time simulated ATC environment was created by means of a combination of simulated ATC facilities and simulated air traffic. Both of these simulations were provided by the FAA and created the environment in which the SST simulator was operated for the tests. (See refs. 4 and 5.)

The simulated ATC facilities were staffed by experienced air traffic controllers. (See fig. 3.) All control positions were provided with modern display and communication

equipment including display of aircraft target symbols and target identification and altitude tags (alpha-numeric displays). Controllers were also provided with flight-path extrapolation capability (based on projection of current aircraft performance) and capability of "blinking" a target symbol as an attention device for "handoff" (transfer of a target to another controller). The controller's equipment was considered to be representative of the alpha-numeric system planned for 1970. (See refs. 4 and 5.)

The simulated air traffic was created by 108 electronic radar target generators (fig. 4), each programed to have the generalized flight characteristics of a particular type of aircraft. The traffic sample included propeller, subsonic jet, and SST airplanes. Each target generator was operated by a "pilot" who maneuvered a spot of light, representing the aircraft position, along the airways map at the top of the console and on climb and descent profiles by means of a control panel according to a programed script and instructions from the air traffic controllers received over a simulated radio communication network. The ground-coordinate-position data from the target generators were fed through radar simulators which transformed the data into radar form, that is, properly gated target video pulses and antenna position. The video pulse and antenna data were fed to the controllers' displays to provide the traffic sample.

#### Data Transmission and Communications

Data transmission and communications between the SST simulator and the simulated ATC facilities were effected over telephone lines. The SST simulator ground coordinate and altitude data and radar beacon transponder signal were transmitted by a data phone link. Communications between the SST simulator pilots and the controllers were effected over private telephone lines which were connected into a special telephone system used for communications between target generator pilots and controllers. The special telephone system allowed all pilots to make connections with the same controller simultaneously; thus, the interference of actual radio communications was simulated.

### TEST PROGRAM

#### General

The test program was designed to study departure and arrival operations under IFR conditions into and out of John F. Kennedy and Los Angeles International Airports (JFK and LAX). The test environments and route structures used are shown in figure 5. The route structures, representing FAA concepts for the 1970 to 1975 time period, consisted of the present-day airway structure at altitudes below about FL 400 and parallel one-way track systems at the higher altitudes.



The traffic samples used at NAFEC included current propeller-driven and subsonic jet aircraft types as well as a number of supersonic aircraft. In these traffic samples, the average number of supersonic aircraft operations per hour varied between 15 and 52. The SST airplanes represented in these traffic samples were the Anglo-French design and the same two United States design study configurations used in the SST simulator. The U.S. design study configuration with a double-delta wing was used in the tests at JFK, and a U.S. design study configuration with a variable-sweep wing was used in the tests at LAX. The traffic samples in the LAX operations also included representations of forthcoming large subsonic jet aircraft such as the Lockheed C5A and Boeing 747 and military supersonic aircraft. Movements of propeller-driven and subsonic jet airplanes were based on current peak hour traffic figures for the area. Movements of other types of aircraft were based on estimated peak traffic figures for the 1970 to 1975 time period.

All traffic was under the positive control of en route or terminal area control facilities. ATC, aircraft, and airport equipment considered to be representative of the 1970 to 1975 time period were simulated. A more complete description of the test program is given in references 4 to 6.

### SST Operating Procedures

The SST simulator was operated by captain and first officer teams from Trans World Airlines and United Air Lines. The crews included pilots in airline supervisory and management positions as well as those engaged in full-time scheduled airline operations. Airline experience of crew members varied from 8 years (4000 flight hours) to 28 years (22 000 flight hours).

Departures were initiated just prior to scheduled departure time by a radio call by the first officer to ATC departure control for clearance instructions. The departure operation was generally ended when cruise conditions had been established. Arrivals were initiated in cruising flight by a radio call from the first officer giving an estimated time of arrival over a prescribed location. The arrival operation was concluded at touch-down on the runway. For some departures and arrivals, the SST was operated in cruising flight for periods up to about 20 minutes, by using either cruise-climb or step-climb procedures.

The climb and descent schedules and the engine, buffet, structural, and sonic-boom overpressure limitation boundaries for SST configurations A and B are shown in figures 6 and 7. For each configuration, separate schedule and limitation figures are given for oceanic (international version) and domestic operations (parts (a) and (b), respectively, of figs. 6 and 7) because of the variation in climb schedules and buffet boundaries associated with weight and allowable sonic-boom overpressure level differences. For the oceanic departures with configuration A, the sonic-boom overpressure limit was eliminated as an

operating restriction; and the airplane was flown along the maximum allowable operating speed structural boundary  $V_{MO}$ . For the oceanic departures with configuration B, a sonic-boom overpressure limit of 2.5 lbf/ft<sup>2</sup> (119.7 N/m<sup>2</sup>) was prescribed. For both configurations on overland departures, the sonic-boom overpressure level was restricted to 2.0 lbf/ft<sup>2</sup> (95.7 N/m<sup>2</sup>). For some of the domestic departure operations, transonic acceleration was delayed by a subsonic-speed level-flight operation at FL 310 to a designated en route point in order to place the superboom (the amplified sonic boom created during transonic acceleration (ref. 7)) in an area of low population density. The descent schedule for both configurations consisted of a slowup segment at or near cruise altitude followed by a constant indicated airspeed descent. For configuration A, because of the higher final cruise altitude, a descent to FL 670 was necessary prior to the slowup phase in order to insure sufficient cabin pressurization capability with engines in the flight idle condition.

The thrust and configuration schedules and operating procedures used in the climb and descent operations for both SST configurations are given in the appendix as excerpts from the check list form supplied to the crew. In addition to the procedures specified in the check lists, thrust was reduced after take-off as required to hold the airspeed between 200 and 250 KIAS during maneuvering in the terminal area. For configuration A, the spoilers and flaps were used on occasion at subsonic speeds to expedite the descent. For both configurations, inflight thrust reversal (available at subsonic speeds) was used on a very few occasions to expedite the descent. In all the descents, reduction in speed to 250 KIAS was made on approach to the terminal area and to lower airspeeds as requested by the air traffic controllers.

The aircraft simulator was flown by manual control entirely (no autopilot). The flight director system was used to provide horizontal and vertical flight-path guidance. For the vertical guidance along the various climb and descent profiles, the flight director element of the attitude indicator – programed to display the pitch input required to return to the Mach number altitude schedule – was employed. For configuration A, the wing-sweep angle was controlled manually by using the wing-sweep program shown in figure 8.

### ATC Procedures

In general, for the portions of the departures and arrivals during which the SST was at subsonic speed (below about FL 400), present-day ATC procedures for control of air traffic (ref. 8) with no preferential treatment for SST airplanes were used. The standard instrument departure (SID) and terminal arrival routes were the same or similar to those used in present practice. (See fig. 9.) All aircraft were subject to step-climb and step-descent operations associated with SID altitude restrictions and hand-off (controller-to-controller transfer) procedures. For arriving aircraft, the usual speed-control

procedures of reduction to 250 KIAS at 30 nautical miles (55.6 kilometers) from the airport and controller-requested speed changes for spacing purposes were employed. Radar vectoring was used by the controllers to shorten standard instrument departure and arrival routes when traffic conditions permitted. Standard subsonic jet transport holding procedures were used for the SST. A conventional holding speed of 250 KIAS was used; however, holding was done at altitudes of 15 000 feet (4.58 km) up to about 30 000 feet (9.15 km).

For flight at supersonic speeds, some special ATC handling procedures based on results from the initial investigations in this program were specified. (See refs. 2 and 3.) Flight at supersonic speeds was specified along one-way track systems. (See fig. 5.) For transitioning between the basic airway system and the parallel track system, various arrangements involving existing navigation aids, radar vectors, and fan track systems were used. Conflicts between climbing and descending SST airplanes at altitudes above FL 350 were resolved, if possible, by vectoring or leveling the descending aircraft to avoid interrupting the transonic acceleration phase of the climbing SST. Holding or circling maneuver instructions were not permitted to be given to aircraft operating at supersonic speeds. A more complete description of ATC procedures employed is given in references 4 and 5.

## RESULTS AND DISCUSSION

Operating practice results obtained from the departure and arrival operations with both SST configurations are presented in figures 10 to 12 and figures 13 to 19. These results cover climb and descent performance, operating speed practices, and overspeed events. The climb and descent performance results include examples of airplane pitch attitude, flight-path angle, and vertical speed; time at various altitudes and Mach numbers; and use of thrust augmentation in climb. The operating-speed-practice results are for the forebody, landing gear, flap, variable-sweep wing, and spoiler. Overspeed event results are given for cruise as well as for climb and descent operations.

### Climb and Descent Performance

Typical results. - Values of airplane pitch attitude  $\theta$ , flight-path angle  $\gamma$ , and vertical speed  $\dot{h}$ , selected from time histories of typical climb and descent operations are given in figure 10 as a function of Mach number  $M$  for SST configuration A. Also shown are the calculated maximum values of flight-path angle for unaccelerated flight in the clean configuration corresponding to the thrust-drag relationships for the thrust schedules for climb and descent given in the appendix. Results are given from both domestic and oceanic operations. For the two operations, the relationships of  $\theta$ ,  $\gamma$ , and  $\dot{h}$  with  $M$  are very similar.

In the climbs, the increase in the performance quantities from zero values to those shown at  $M \approx 0.30$  ( $\theta$  approximately  $18^\circ$ ) occur during the aircraft rotation at take-off. Reduction of these quantities at  $M \approx 0.35$  ( $\theta$  to about  $11^\circ$ ) reflects the power reduction made for maneuvering in the terminal area. The increase in values at  $M \approx 0.40$  (to  $\theta$  values of  $16^\circ$  to  $18^\circ$ ) results from application of climb power and resumption of climb. Over the Mach number range from about 0.40 to 2.25, the reduction in the values of  $\theta$ ,  $\gamma$ , and  $\dot{h}$  result from the loss of excess thrust available with increase in speed and the use of the excess thrust for acceleration rather than climb. The constraint on performance imposed by the sonic-boom overpressure limitation is evident by comparison of the  $\gamma$  and  $\dot{h}$  values at supersonic speeds for the domestic operation (fig. 10(a))

( $\Delta p = 2.0 \text{ lbf/ft}^2$  ( $95.7 \text{ N/m}^2$ )) with the oceanic operation (fig. 10(b)) ( $V_{MO}$  climbout, see fig. 6). The increase in the climb and acceleration capability at Mach numbers above about 2.25 arises from an increase in excess thrust which occurs beyond  $M \approx 2.0$ , and the reduction in use of excess thrust for acceleration which is inherent in the constant airspeed climb scheduled for this Mach number range. (See fig. 6.) The final values of  $\theta$ ,  $\gamma$ , and  $\dot{h}$  shown at  $M = 2.7$  represent initial cruise conditions.

For the descents, the values of  $\theta$ ,  $\gamma$ , and  $\dot{h}$  shown at  $M = 2.7$  are those for final cruise conditions. The variations in these quantities with  $M$  basically show the effects of the operating practices associated with the descent schedule. (See fig. 6.) The level-flight slowdown between  $M = 2.5$  and 1.8 resulted in the highest values of  $\theta$  during the descent (from  $7.5^\circ$  to  $8.5^\circ$ ) because of the high angle of attack required for level flight at 67 000 feet (20.4 km) at  $M = 1.8$ . The values of  $\gamma$  and  $\dot{h}$ , which, in general, increased with decrease in speed through the supersonic speed range to values of about  $-5^\circ$  and  $-5500 \text{ ft/min}$  ( $1.68 \text{ km/min}$ ) at about sonic speed, decreased with further reduction in speed because of the increased lift-drag ratio resulting from the wing-sweep change from  $72^\circ$  to  $42^\circ$ . The variations in the values of  $\theta$ ,  $\gamma$ , and  $\dot{h}$  at subsonic speeds reflect flap and spoiler operations which are discussed in a subsequent section.

Time at various altitudes and Mach numbers. - The average time spent at various altitudes and Mach numbers during the climb and descents of some typical departure and arrival operations are shown in figures 11 and 12. The results are presented as histograms of the amount of time spent in increments of 5000-foot (1.52 km) altitude and in increments of 0.5 Mach number. The altitude-time results are for SST configuration B in domestic departures from and domestic and oceanic arrivals to JFK on the route structures shown in figure 5. Each of the altitude-time histograms is based on the average of data from 2 to 7 departures or arrivals. The results for Mach number as a function of time are for SST configuration A for both domestic and oceanic arrivals and departures to and from LAX on the route structures shown in figure 5. Each of these histograms is based on the average data from 6 to 20 arrivals or departures. Both

altitude-time and Mach number time results are included from domestic departures in which the amplified sonic boom created during transonic acceleration (superboom) was placed in the arbitrarily selected low-population areas shown in figure 20.

Comparison of the altitude-time results for the standard domestic departures (unplaced superboom) on the two routes (fig. 11(a)) indicates that the time spent in the various altitude increments was about the same except for the 0- to 5000-foot (1.52 km) increment. The approximately 7 extra minutes spent in the 0- to 5000-foot (1.52 km) altitude increment for the departure on route Upper South 1 to Upper West 5 compared with the departure on Upper West 4 (these routes are shown in fig. 5(b)) occurred because of a 4000-foot (1.22 km) altitude restriction required on the SID for this route for separation from crossing oceanic arrival traffic at 6000 feet (1.83 km). (See figs. 9(a) and 9(b).) Placement of the superboom resulted in an increase of about 11 minutes on the Upper West 4 route and about 7 minutes on the Upper South 1 to Upper West 5 route in the time spent in the 30 000-foot to 35 000-foot (9.15 km to 10.68 km) altitude range. The relatively long period spent in the 50 000-foot to 55 000-foot (15.2 km to 16.8 km) altitude range for all departures resulted from the detrimental effect on performance imposed by the climb schedule required to observe the sonic-boom overpressure level of  $2.0 \text{ lbf/ft}^2$  ( $95.7 \text{ N/m}^2$ ). The altitude-time results for the arrivals show that about 3 minutes were required for the slowdown at cruise altitude before descent was initiated. Comparison of the domestic and oceanic arrivals indicates that the time spent at various altitudes was about the same except below about 15 000 feet (4.57 km). The larger amount of time spent at these altitudes for the oceanic arrivals resulted from a longer distance from the holding location to the runway (figs. 9(a) and 9(b)) and from the route-lengthening effect of the 6000-foot (1.83 km) altitude restriction for separation of departure traffic.

For the operations with SST configuration A at LAX (fig. 12), comparison of the average time spent at Mach numbers above 1.0 for the domestic departures with the oceanic departures shows the detrimental effect on performance of the climb schedule limited by the sonic-boom overpressure level of  $2.0 \text{ lbf/ft}^2$  ( $95.7 \text{ N/m}^2$ ) compared with the  $V_{MO}$  climb schedule. About 8.5 minutes more was spent on the average at supersonic speeds in the standard domestic (unplaced superboom) departures than in the oceanic departures, and most of this additional time was spent in the Mach number range from 1.0 to 1.5. Placement of the superboom in the LAX domestic departures resulted in about 9 extra minutes in the Mach number range from 0.5 to 1.0. The results showing the average time at various Mach numbers for the arrivals emphasizes the relatively greater amount of time spent at subsonic speeds compared with supersonic speeds in descents. The larger amounts of time at subsonic speed reflects operations at reduced speeds for ATC spacing and to observe terminal area speed restrictions, and the time

required for terminal-area navigation involved with aircraft separation, sequencing, and runway alinement.

Use of thrust augmentation. - The average climb time and the average time that full-thrust augmentation power was used during climb with SST configuration A in the LAX departures is given in table IV. Climb time is defined as the period from lift-off until initial cruise was established. Final thrust augmentation was used continuously from about 31 000 feet (9.45 km) until power was reduced just below 67 000 feet (20.4 km) in establishing initial cruise conditions.

Less thrust augmentation time was required in the placed superbomb departures than in the unplaced superbomb departures since the aircraft weight was less during the supersonic speed climb portion of the placed superbomb departures because of the fuel burned in the approximately 10 minutes of subsonic speed operation at 31 000 feet (9.45 km). The use of the more efficient climb schedule corresponding to  $V_{MO}$  for the oceanic departures in contrast to the use of the sonic-boom overpressure-limited climb schedule for the domestic departures explains the smaller thrust-augmentation use time for the oceanic departures compared with that of the domestic departures.

#### Operating Speed Practices

Forebody and landing gear - configuration B. - Forebody and landing-gear operating speed practices during the climb and descent phases of the simulated departure and arrival operations are shown for SST configuration B (fixed geometry) in figure 13. The results are presented as histograms of the number of occurrences for 5-knot airspeed increments of the maximum recorded airspeed with the forebody deflected (fig. 13(a)) and the landing gear extended or actuating (fig. 13(b)). Also given are the maximum allowable operating airspeeds in these configurations (speed placards). The histograms represent results from 60 climbs and 39 descents. For this SST configuration, the forebody could be placed in three positions - fully deflected, intermediate, and retracted. The results given in figure 13 for the forebody are for the fully deflected condition only.

The results given in figure 13 show that for the climbs, the placard speeds were exceeded with the forebody fully deflected or the landing gear extended, only once in each case, by 10 KIAS for the forebody, and by 25 KIAS for the landing gear. For those climbs in which the placard speeds were not exceeded, the margins between the maximum operating speed and the placard speed varied from 20 to 85 KIAS for the forebody and from 5 to 80 KIAS for the landing gear. The most probable speed margins were about 45 KIAS for the forebody and 35 KIAS for the landing gear. These operating-speed practices in the climbs were basically determined by the take-off speed requirements and by piloting procedures. For this SST configuration, rotation speed in take-off was 150 KIAS. Lift-off generally occurred in the range of speeds from 180 to 200 KIAS. The pilots raised the

landing gear first and the forebody immediately after. The lower speed margin on the average for the landing gear compared with the forebody is associated with the 12-second retraction time for the landing gear whereas the simulated retraction time of the forebody was practically instantaneous. A retraction time for the forebody was not represented in these tests since design retraction-time data were not available.

In general, for the climb operation the speed placard of 250 KIAS for the forebody in the fully deflected position required that the forebody be retracted to the intermediate position almost immediately after take-off. For the forebody, the placard speed in the intermediate deflected position was 325 KIAS; thus, the forebody had to be fully raised in order to climb at the scheduled speed in the subsonic phase of climb (340 KIAS, see fig. 7). The pilots commented that from an operational viewpoint, it would appear desirable to have a placard speed for the forebody high enough to allow the forebody to remain fully deflected throughout the subsonic portion of the climb. Such an arrangement would eliminate the complication of retraction to an intermediate position immediately after take-off and would provide increased visibility throughout operations in the high-traffic-density airspace.

In the descents, the placard speed in the forebody-deflected condition was exceeded six times by increments in speed up to 30 KIAS. For these descents with configuration B, a scheduled speed for deflection of the forebody was not specified; the margin between allowable speed for deflection and the placard speed was therefore zero. The relatively large percentage of cases for which the placard speed was exceeded with the forebody deflected is thought to result from a placard speed lower than the scheduled descent speed (see fig. 7) and of the same value as the maximum speed allowable by ATC regulation in the terminal area. The pilots again commented that from an operational standpoint, a higher placard speed appeared to be desirable to allow high-speed descents with the increased visibility available with the forebody deflected.

For the landing-gear-down condition in the descents, the placard speed was exceeded six times, by increments in speed up to 20 KIAS. There were also seven occurrences in which the increments in the margin between the maximum operating speed with the gear down and the placard speed was 15 KIAS or less. Because SST configuration B was not equipped with flaps or spoilers, the landing gear was often extended as a drag-increasing device for slowup or to steepen the descent. Such operations were noted at altitudes up to 15 000 feet (4.57 km). The use of the landing gear as a drag-producing device was apparently the primary cause of the substantial number of occurrences of low-speed margin operation and of exceedance of the placard speed. Although SST configuration B had the capability of inflight thrust reversal at subsonic speeds, this method of steepening the descent was used in only six descents. In these cases, the use of thrust reversal ranged from 2 to 6 minutes in any one descent and occurred at altitudes from as

high as 39 000 feet (11.9 km) to as low as 2000 feet (0.61 km). The general use of deflected landing gear rather than thrust reversal for slowup or for steepening the descent probably stemmed from the pilot's previous operational experience. These results indicate that for SST configurations without drag-producing devices such as flaps or spoilers, a landing-gear placard speed greater than the scheduled descent speed would be desirable.

Forebody, landing gear, and flap – configuration A. - Forebody, landing gear, and flap operating-speed practices during the climb and descent phases of the simulated departure and arrival operations are shown for SST configuration A (variable-sweep wing) in figure 14 in the same form used for the operating-speed practice results for configuration B in figure 13. The histograms in figure 14 represent results from 58 climbs and 30 descents. The operating-speed practices for the forebody are shown in figure 14(a). The placard speed for the forebody was  $M = 0.90$ , and the scheduled speed for retraction in climbs and deflection in descents was  $M = 0.85$ . For this SST configuration, three placard speeds were specified for the landing gear: (1) 320 KIAS for the down and locked condition (doors closed), (2) 250 KIAS during the retraction cycle, and (3) 270 KIAS during the extension cycle. The operating-speed practices for the landing gear are shown for each of the three operating conditions in figures 14(b), 14(c), and 14(d). For the flaps, placard speeds of 290 and 225 KIAS were specified for flap-deflected configurations of  $5^\circ$  and  $40^\circ$ , respectively. The operating-speed practices for the flap-deflected configurations are given in figures 14(e) and 14(f).

The operating-speed-practice results for the forebody (fig. 14(a)) indicate that for most of the climbs and descents, the forebody was operated within a Mach number increment of  $\pm 0.05$  of the scheduled speed for operation. Because a retraction time for the forebody was not simulated in these tests because of lack of design data, the actual speed margins for the climbs would be less than those indicated. (Calculations for the climbing condition at approach to the forebody placard speed indicate that the speed margins shown would be reduced by about  $0.01M$  for each 14 seconds of retraction time.) In seven climbs and three descents, the placard speed was exceeded, by increments in Mach number up to 0.15 in the climbs and 0.03 in the descents. The cases in which the placard speed was exceeded in the climbs resulted from pilot inattention to the flight-procedure check list – in some cases because of distraction by other duties. The cases in which the placard speed was exceeded in the descents resulted from inadvertent increases in speed after the forebody had been lowered at the scheduled speed for operation. These results indicate that an aural warning is needed in addition to the forebody warning light to call to the attention of the crew that the forebody placard speed has been exceeded.

The operating-speed practice results for the landing gear (figs. 14(b), 14(c), and 14(d)) indicate, in general, substantial speed margins between the operating speeds and



the placard speeds for all three landing-gear conditions (extended, retracting, and extending). The placard speeds were not exceeded while in these configurations in either climb or descent operations. In the climbs, the most probable speed margins are shown to be 145 KIAS (gear extended) and 75 KIAS (gear retracting); in the descents, the most probable speed margins are shown to be 140 KIAS (gear extended) and 90 KIAS (gear extending). The relatively larger speed margins for this SST configuration compared with SST configuration B (fig. 13) are believed to be associated with both the higher placard speeds for this configuration and little use of the landing gear as a drag device in descents. For this configuration, spoilers and flaps were available at subsonic speeds (as well as inflight thrust-reversal capability) for expediting the descent.

The operating-speed-practice results with the flap deflected (figs. 14(e) and 14(f)) indicate sufficient speed margins between the maximum recorded speeds and the placard speeds for climb operations for both flap-deflected configurations. The most probable speed margins are seen to be 85 KIAS for the 5° flap-deflected configuration and 55 KIAS for the 40° flap-deflected configuration. For the descent operations, the maximum recorded speeds with flaps deflected extended over a wide range of speeds. With the flaps deflected 5°, the maximum recorded speeds approached within about 10 KIAS of the placard speed. With the flaps deflected 40°, the placard speed was exceeded in eight arrivals. The incidents in which the placard speed was exceeded by about 50 and 70 KIAS both occurred at low altitude during the maneuvering from the downwind leg of the approach to the final approach direction and resulted from application of high amounts of thrust for periods of about 30 and 130 seconds, respectively. In both cases, the overspeeding appeared to result from misjudgment of the thrust required for the maneuver and the high concentration required in navigating the airplane during these periods. The other incidents in which the placard speed was exceeded in the descents with flaps deflected 40° resulted upon deflection of the flaps from the 5° position at speeds above the placard speed. These flap changes occurred in the terminal area and apparently were used primarily for slowups and, in some cases, to expedite descent. The wide range of speeds over which the SST was operated with the flaps deflected 5° in the descents appeared to result from the use of the flaps to expedite descent. The use of flaps and spoilers in descent is discussed in a later section.

Variable-sweep wing – configuration A. - For SST configuration A, the maximum Mach numbers to which the airplane was operated in the climbs with  $\Lambda = 30^\circ$  and  $\Lambda = 42^\circ$  and the minimum Mach numbers to which the airplane was operated in the descents with  $\Lambda = 72^\circ$  are shown in figure 15. Also shown are the scheduled altitude and Mach numbers for wing-sweep changes and the maximum operating limit Mach numbers ( $M_{MO}$ ) for each sweep angle. The prescribed wing-sweep-angle program for climb and descent operations is given in figure 8. However, in the climbs, the wing-sweep

change from  $30^\circ$  to  $42^\circ$  was scheduled at 3000-foot (0.915 km) altitude as shown in figure 15 instead of at  $M = 0.35$  as shown in figure 8. This change was made so that this wing-sweep operation could be performed at the reinitiation of climb following the take-off noise-abatement procedure, in an attempt to simplify the climb task for the crew. A restriction was placed on wing-sweep operations during the accelerated conditions existing in turns. The curve labeled "overspeed warning" in figure 15 defines the Mach number altitude relationship equivalent to the  $V_{MO} + 6 \text{ KIAS}$  function (based on  $V_{MO}$  values for  $\Lambda = 42^\circ$  and  $\Lambda = 72^\circ$ ) used to actuate the aural and visual overspeed warning indicators.

For the climbs, the altitudes which were reached with the wing still in the  $30^\circ$  sweep position were generally above the scheduled altitude for initiating the sweep to  $42^\circ$ . For those departures in which little maneuvering was required after take-off, the wing-sweep change was usually initiated at or near the scheduled altitude. However, for most of the departures, considerable maneuvering was required and the initiation of the wing-sweep change was apparently delayed because of the restriction on wing-sweep operation in turning flight and also because of crew involvement with other tasks. In many of the climbs, the scheduled Mach number for sweeping the wing from  $42^\circ$  to  $72^\circ$  was also exceeded. In the descents, however, the wing-sweep change from  $72^\circ$  to  $42^\circ$  was always made at or below the scheduled Mach number. Overspeeding beyond the  $M_{MO}$  occurred in a number of the climbouts – in three cases with  $\Lambda = 30^\circ$  and in eight cases with  $\Lambda = 42^\circ$ . In two cases (not shown), overspeeds with  $\Lambda = 42^\circ$  (at  $M = 0.92$  and  $1.00$ ) occurred at altitudes above 25 000 feet (7.61 km) in the descents, both incidents being associated with leveling operations. Presumably, these overspeeds in both climbs and descents might not have occurred if the overspeed warnings had been based strictly on the  $V_{MO}$  for the existing  $\Lambda$  rather than on the simplified overspeed warning based only on the  $V_{MO}$  for  $\Lambda = 42^\circ$  and  $\Lambda = 72^\circ$  (fig. 15) which was used. However, the considerable number of occasions in climb in which the wing-sweep change was delayed beyond the scheduled altitude or Mach number shows the need for a wing-sweep warning device to remind the crew to comply with the wing-sweep schedule.

### Flap and Spoiler Operations in Descent

The results for a number of descents given in figure 16 show the histories of the portion of the altitude-speed profiles (fig. 16(a)) over which the flap was deflected to the  $5^\circ$  configuration and (fig. 16(b)) over which the spoilers were extended. The results are taken from a sample of 27 descents. The flap was deflected in 20 of the descents and the spoilers were extended in 6 of the descents. Also shown are the flap placard speed and the maximum operating speed  $V_{MO}$ . The placard speed for the spoilers was equal to  $V_D$ . If all descents are considered, the pilots used the flaps and spoilers over nearly the

entire altitude range corresponding to subsonic speed flight. However, the placard speeds for the 5° flaps and the spoilers were not exceeded in any descents.

The pilots apparently, in general, initially used the flaps and spoilers to slow up to about 250 KIAS, the airspeed required by ATC for operations within 30 nautical miles (55.5 km) of the airport. Continued use of the flaps and spoilers after slowup was to expedite the descent by increasing the descent angle. The necessity for using a drag-producing device to increase the descent angle is illustrated in figure 17. Shown by the dashed line in figure 17 is the  $(T - D)/W$  ratio for descent along the standard descent profile (fig. 6) with the engines in the flight idle condition and the aircraft in the clean condition. The negative values of  $(T - D)/W$  indicate that the drag is greater than the thrust. Since the slowdown and descent capability is directly a function of the amount that the drag exceeds the thrust, the  $(T - D)/W$  values shown by the dashed line indicate that the slowdown and descent capability decreases by about one-half during the slowdown from supersonic to subsonic speeds. To compensate for the loss in slowdown and descent capability at subsonic speeds, the pilots, in most descents, deflected the flaps and spoilers to increase the drag. The values of  $(T - D)/W$  obtained with the flaps and spoilers deflected are shown by the solid lines in figure 17.

#### Overspeed Events

Climb and descent. - Overspeed events (incidents where  $V_{MO}$  was exceeded by 6 KIAS or more) during the climb and descent operations are shown in figure 18 for both SST configurations in terms of the maximum airspeeds reached at the altitude at which the overspeed occurred. The climb and descent schedules, the overspeed boundaries (in terms of  $V_{MO} + 6$  KIAS, the overspeed warning limit), and the design speed limit  $V_D$  boundaries are also shown. The results for SST configuration A are from 12 climbs and 10 descents; the results for SST configuration B are from 55 climbs and 38 descents. For the oceanic departures with configuration A, no restriction was placed on the sonic-boom overpressure level so that most of the oceanic climbs were made along the  $V_{MO}$  profile. The remainder of the oceanic climbs with configuration A and all the oceanic climbs with configuration B were made along climb schedules designed to limit the sonic-boom overpressure level to 2.5 lbf/ft<sup>2</sup> (119.7 N/m<sup>2</sup>). For both configurations, the domestic climbs were made along 2.0 lbf/ft<sup>2</sup> (95.7 N/m<sup>2</sup>) sonic-boom overpressure limited schedules, and the descents were made along schedules limiting sonic-boom overpressure values to about 1.5 to 1.7 lbf/ft<sup>2</sup> (71.8 to 81.4 N/m<sup>2</sup>).

For configuration A, overspeeding incidents occurred 16 times in the 12 climbs and 13 times in the 10 descents. For configuration B, overspeeding incidents occurred 38 times in the 55 climbs and 32 times in the 38 arrivals. For both configurations, most of the overspeeds above  $V_{MO}$  were 20 KIAS or less; however, a few overspeeds slightly

over 30 KIAS were noted. The overspeeds occurred over the speed-altitude ranges where the climb and descent schedules were the same as or close to the  $V_{MO}$  boundary. A number of the overspeeds occurred in the process of making the transition from climbing to cruising conditions. At altitudes between 30 000 and 35 000 feet (9.15 and 10.68 km), the overspeed incidents are connected with the scheduled power increase at 31 000 feet (9.45 km) from the power for climb at subsonic speeds to the maximum augmented-power condition required for transonic acceleration and climb at supersonic speeds. Most of the other overspeeds in climb happened in the altitude range from 5 000 to 18 000 feet (1.52 to 5.48 km) as a result of the process of accelerating to the climb-schedule speed from a low-speed climb. A climb speed lower than the scheduled value was generally used at the lower altitudes: With one exception (an overspeed at initiation of descent with configuration B), the overspeeds in descents occurred below 30 000 feet (9.15 km), where the descent schedule was the same as  $V_{MO}$ . There were fewer overspeeds below 15 000 feet (4.57 km) than above because of the usual slowup to the terminal area air-speed of 250 KIAS which was generally effected in this altitude range. The overspeed results shown, similar to the results presented in reference 9, indicate a need for the climb and descent schedules to be at least 10 to 20 KIAS less than the  $V_{MO}$  boundary in order to prevent frequent overspeed incidents.

Cruise.— Overspeeding results from 9 hours of cruise operations obtained by summation of short periods of cruise (of about 20 minutes each) preceding descent in the arrival operations at New York with configuration B are given in figure 19. Manual control was used for cruise-climb procedures under calm-air standard atmospheric conditions. In general, the pilots used a sensitive (5 to 1) pitch-attitude indicator for assistance in vertical flight-path control and a slow-fast indicator for assistance in speed control. Both indicators were integral elements of the attitude-director indicator. For these operations, the overspeed warning was activated at  $M = 2.71$ . The results, based on 111 overspeeding incidents, are presented in terms of the probability of exceeding the cruise Mach number of 2.7 by various increments in Mach number. The results show that the overspeed warning increment in Mach number used ( $\Delta M = 0.01$ ) was exceeded about 50 times in each 100 overspeed incidents. A more reasonable overspeed warning increment of 0.035 in Mach number (equivalent at cruise conditions to the 6 KIAS overspeed warning used in subsonic jet operations) would apparently be exceeded only 4 times in each 100 overspeed incidents. The maximum overspeed Mach number increment measured was 0.05, which is equivalent to about 10 KIAS for these flight conditions.

Examination of the time-history records of the motions of this SST configuration in the cruise-climb operations indicated that the overspeeds were connected with a phugoid oscillation with a period of about 5 minutes. The pilots were forced to monitor the speed continuously and to make throttle adjustments on the order of one every 3 to 5 minutes.

## CONCLUDING REMARKS

Operating practices of the supersonic transport (SST) during simulated operations in air-traffic control (ATC) system environments conceived for the time period for introduction of the SST into service have been presented. An SST flight simulator and the Federal Aviation Administration ATC simulation facilities were used to create the real-time simulations. The aircraft flight simulator was operated by airline crews and the ATC simulation facilities by experienced air-traffic controllers. The test program included departure and arrival operations under instrument flight rule conditions in the New York and Los Angeles terminal areas with two design study configurations of the SST. The design study configurations were representative of variable-sweep and fixed-wing designs. Both designs had variable-incidence forebodies. The principal results are:

1. The number of occasions in which the forebody placard speed was exceeded with the forebody deflected in both climbs and descents with both SST configurations indicated a requirement for an aural overspeed warning in addition to the overspeed warning light. The pilots commented that the forebody placard speed should be high enough to allow the forebody to be fully deflected for all subsonic speed operations.

2. For the variable-sweep-wing SST, flaps and spoilers were often used at subsonic speeds in descents because of the low slowup and descent-angle capability of the clean configuration. The flap placard speed was exceeded on occasion when the flaps were deflected to the landing configuration for these purposes.

3. For the fixed-wing SST (not equipped with flaps or spoilers), the landing gear was often extended as a drag-increasing device for slowup or to steepen the descent; use of the landing gear for these purposes resulted in a number of incidents in which the landing-gear placard speed was exceeded.

4. The crew failed to comply with the wing-sweep schedule on many occasions; thus, a need for a wing-sweep warning device is indicated.

5. For portions of the climbs and descents in which the scheduled speed was close to or equal to the maximum operating limit speed, many of the overspeed events occurred during manually controlled flight. Most of the overspeeds were 20 knots or less; however, a few overspeeds slightly greater than 30 knots were noted.

6. In a total of 9 hours of manually controlled cruising flight under calm-air standard atmospheric conditions, 111 overspeed incidents were noted. The overspeed-warning-actuation speed (maximum operating limit speed plus 6 knots) was exceeded at the rate of about 4 times for each 100 overspeed incidents. The maximum overspeed Mach number

increment measured was 0.05. In cruise flight, pilots were forced to monitor the speed almost continuously and to make throttle adjustments on the order of one every 3 to 5 minutes.

Langley Research Center,

National Aeronautics and Space Administration,

Langley Station, Hampton, Va., November 6, 1968,

720-05-00-04-23.

## APPENDIX

### CREW OPERATING PROCEDURES CHECK LIST

The following excerpts relating to operating practices were taken from the crew operating procedures check list:

#### Configuration A:

##### Pre-taxi:

Gear	Down and locked
Forebody	Down
Flaps	40°
Wing-sweep angle	30°

##### Take-off:

Throttles	Maximum unaugmented thrust
$V_1 = V_R(\theta \approx 20^\circ)$	150 KIAS
$V_2$	190 KIAS

##### After take-off:

Gear	Up
Flaps	5° at 400-foot (122 m) altitude
Initial climb speed	200 KIAS

##### Noise-abatement procedure:

###### At 1500-foot altitude:

Throttles	75 percent speed
Rate of climb	500 ft/min

###### At 3000-foot altitude:

Throttles	Maximum unaugmented thrust
Flaps	Up
Sweep angle	42°

##### Transition to climb schedule:

Throttles	Maximum unaugmented thrust
Pitch attitude	13°

##### Climb:

Climb schedule (flight director)	Select at 340 KIAS
Forebody	Up at $M = 0.85$
72° wing-sweep angle	Select at $M = 0.85$

## APPENDIX

Throttles	Increase thrust gradually starting at M = 0.85 to give maximum augmented thrust at M = 0.95
Cruise:	
Throttles	Set thrust for M = 2.7 or 500° F
Descent:	
Throttles	Flight idle
42° wing-sweep angle	Select at M = 1.0
Forebody	Down at M = 0.85
Before landing:	
Gear	Down
Flaps	40°
Throttles	Set for 180 KIAS approach speed
Configuration B:	
Pre-taxi:	
Gear	Down
Forebody	Down
Take-off:	
Throttles	Maximum augmented thrust
$V_1 = V_R(\theta \approx 15^\circ)$	150 KIAS
$V_2$	176 KIAS
After take-off:	
Gear	Up
Initial climb speed	200 KIAS
Throttles	Minimum augmented thrust at 3000 feet (0.92 km)
Transition to climb:	
Throttles	Minimum augmented thrust
Pitch attitude	10°
Forebody	Retraction speed not specified – determined by speed placards
Climb:	
Climb schedule	Select at 330 KIAS
Throttles	Maximum augmented thrust at FL 310
Cruise:	
Throttles	Set thrust for M = 2.7



## APPENDIX

### Descent:

Throttles

Forebody

Flight idle

Extension speed not specified – determined  
by placard speeds

### Before landing:

Gear

Throttles

Down

Set for 180 KIAS approach speed

## REFERENCES

1. Anon.: Tentative Airworthiness Standards for Supersonic Transports. Flight Standards Service, FAA, Nov. 1, 1965; Revision 4, Dec. 29, 1967.
2. Sluka, Andrew L.: ATC Concepts for Supersonic Vehicles – Part I. Rep. No. RD-66-62, FAA, Aug. 1966.
3. Sawyer, Richard H.; McLaughlin, Milton D.; and Silsby, Norman S.: Simulation Studies of the Supersonic Transport in the Present-Day Air Traffic Control System. NASA TN D-4638, 1968.
4. Sluka, Andrew L.: ATC Concepts for Supersonic Vehicles – Part II-1. Rep. No. RD-67-38, FAA, Aug. 1967.
5. Sluka, Andrew L.: ATC Concepts for Supersonic Vehicles – Part II-2. Rep. No. RD-67-47, FAA, Nov. 1967.
6. Sawyer, Richard H.; Silsby, Norman S.; and McLaughlin, Milton D.: Simulation Studies of the Supersonic Transport in Future Air Traffic Control Systems. NASA TN D-4944, 1968.
7. Lansing, Donald L.: Applications of Acoustic Theory to Prediction of Sonic-Boom Ground Patterns From Maneuvering Aircraft. NASA TN D-1860, 1964.
8. Anon.: ATC Procedures. AT P 7110.1B, FAA, Nov. 12, 1964. (With changes to July 1967.)
9. McLaughlin, Milton D.: Simulator Investigation of Maneuver Speed Increases of an SST Configuration in Relation to Speed Margins. NASA TN D-4085, 1967.

TABLE I.- SST CHARACTERISTICS

Configuration	T/W <sub>TO</sub> (*)		Minimum transonic acceleration				Wing loading			
			fps <sup>2</sup>	m/sec <sup>2</sup>	fps <sup>2</sup>	m/sec <sup>2</sup>	psf	N/m <sup>2</sup>	psf	N/m <sup>2</sup>
	International	Domestic	International	Domestic	International	Domestic	International	Domestic	International	Domestic
A (Variable-sweep wing)	0.27	0.31	3.5	1.1	1.3	0.4	75	3590	63	3016
B (Fixed double-delta wing)	.40	.40	2.3	.7	1.6	.5	53	2537	47	2250

\*For maximum unaugmented condition, configuration A; for maximum augmented condition, configuration B.

TABLE II.- SYSTEMS OPERATING AND MONITORING EQUIPMENT

System	Indicator	Warning	Control
Configuration A			
Maximum operating limit speed	V <sub>MO</sub> pointer on airspeed dial	Red light and clacker	None
Wing sweep	Dial pointers (left and right wing positions)	None	Handle with detents for $\lambda = 30^{\circ}$ , $42^{\circ}$ , and $72^{\circ}$
Landing gear	Green lights for each gear down and locked	Red "unsafe" light. Placard speed tag on panel	Two-position handle
Forebody	Amber "up" and "down" lights	Red overspeed light. Placard speed tag on panel	Two-position toggle switch
Trailing-edge flaps	Dial pointer (position)	None	Handle with detents for $0^{\circ}$ , $5^{\circ}$ , and $40^{\circ}$ deflections
Leading-edge flaps	Amber light (flaps extended)	None	Automatic
Spoilers	Amber light (spoilers extended)	None	Two-position handle
Configuration B			
Landing gear	Green lights for each gear down and locked	Red "unsafe" light. Placard speed tag on panel	Two-position handle
Forebody	Dial pointer (up, intermediate, and down position)	Red overspeed light. Placard speed tag on panel	Three-position handle

TABLE III.- PLACARD SPEEDS

System	Configuration	Placard speed
Configuration A		
Landing gear	Retracting	250 KIAS
	Extending	270 KIAS
	Down and locked	320 KIAS
Forebody	Deflected	$M = 0.90$
Flaps	Deflected $5^{\circ}$	290 KIAS
	Deflected $40^{\circ}$	225 KIAS
Wing sweep	$\lambda = 30^{\circ}$	300 KIAS or $M = 0.70$
	$\lambda = 42^{\circ}$	350 KIAS or $M = 0.90$
	$\lambda = 72^{\circ}$	$M_{MO}$ for $\lambda = 72^{\circ}$ (see fig. 16(b))
Spoilers	Deflected	$V_D$ (see fig. 19(a))
Configuration B		
Landing gear	Extending, retracting, or down and locked	250 KIAS
Forebody	Fully deflected	250 KIAS

TABLE IV.- THRUST AUGMENTATION USE IN CLIMB

Type of departure	Number of departures averaged	Average time full-thrust augmentation used, min	Average climb time, min
Domestic (unplaced superboom)	11	25	33
Domestic (placed superboom)	15	22.5	40
Oceanic	6	15	23

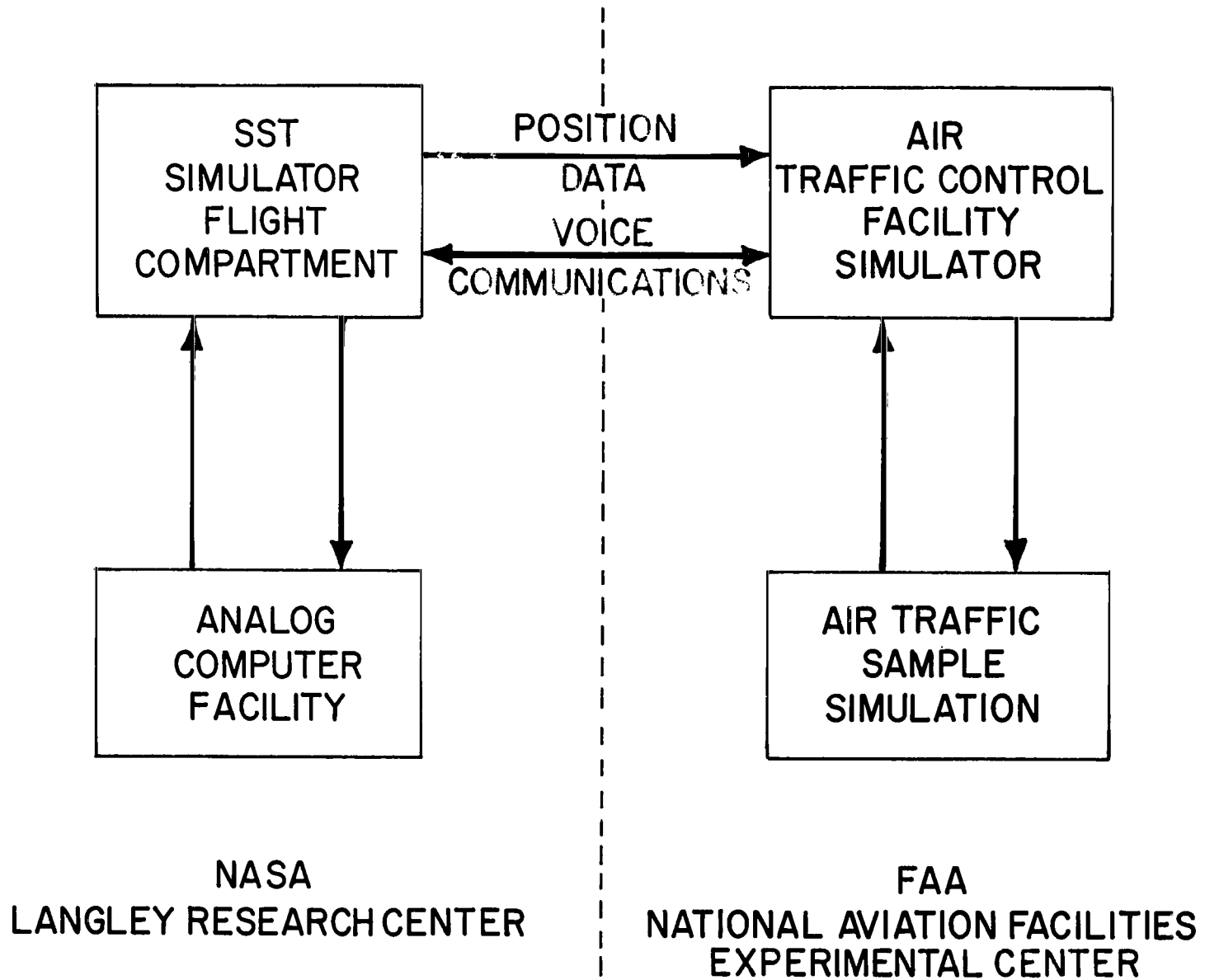
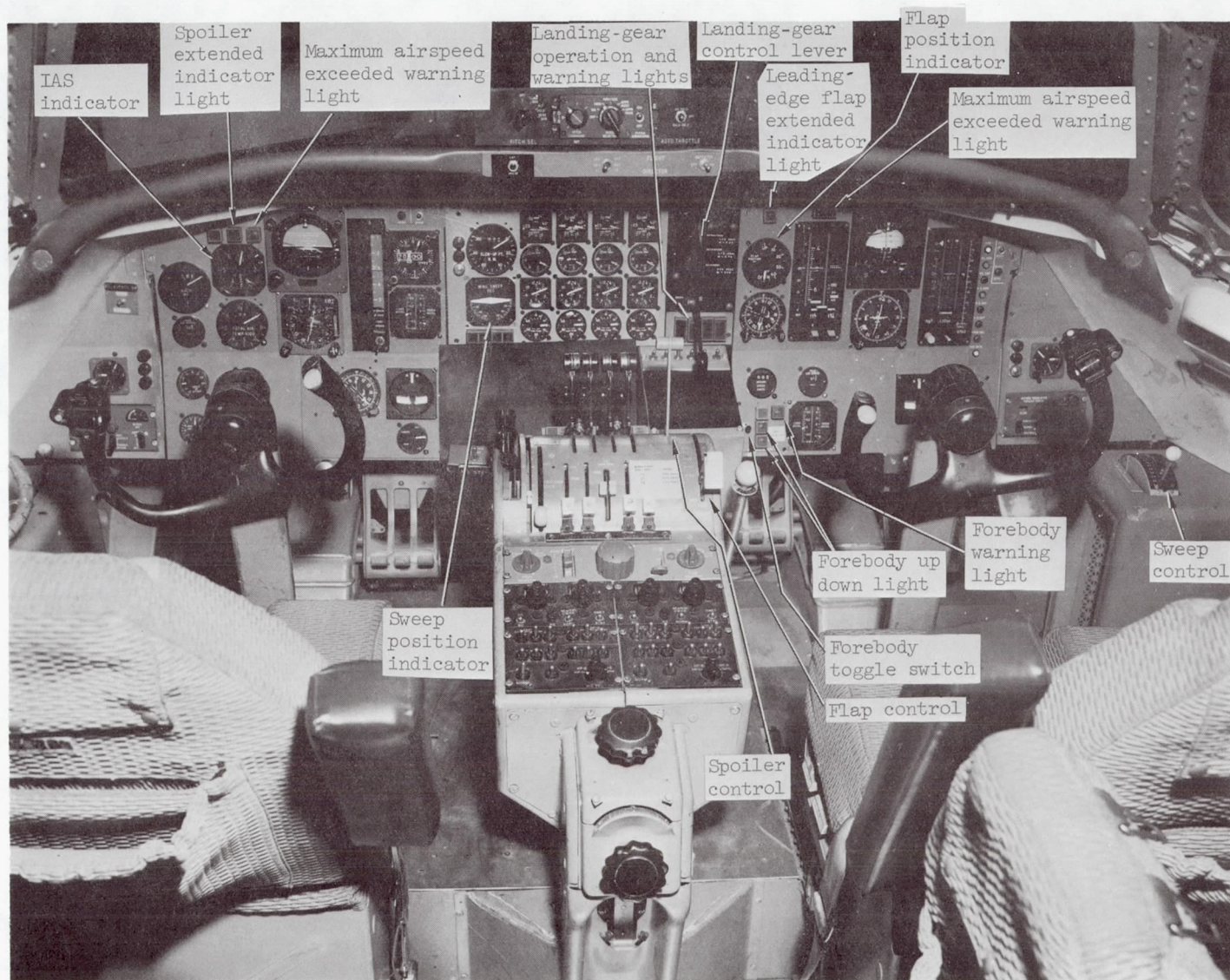


Figure 1.- SST-ATC simulation method.

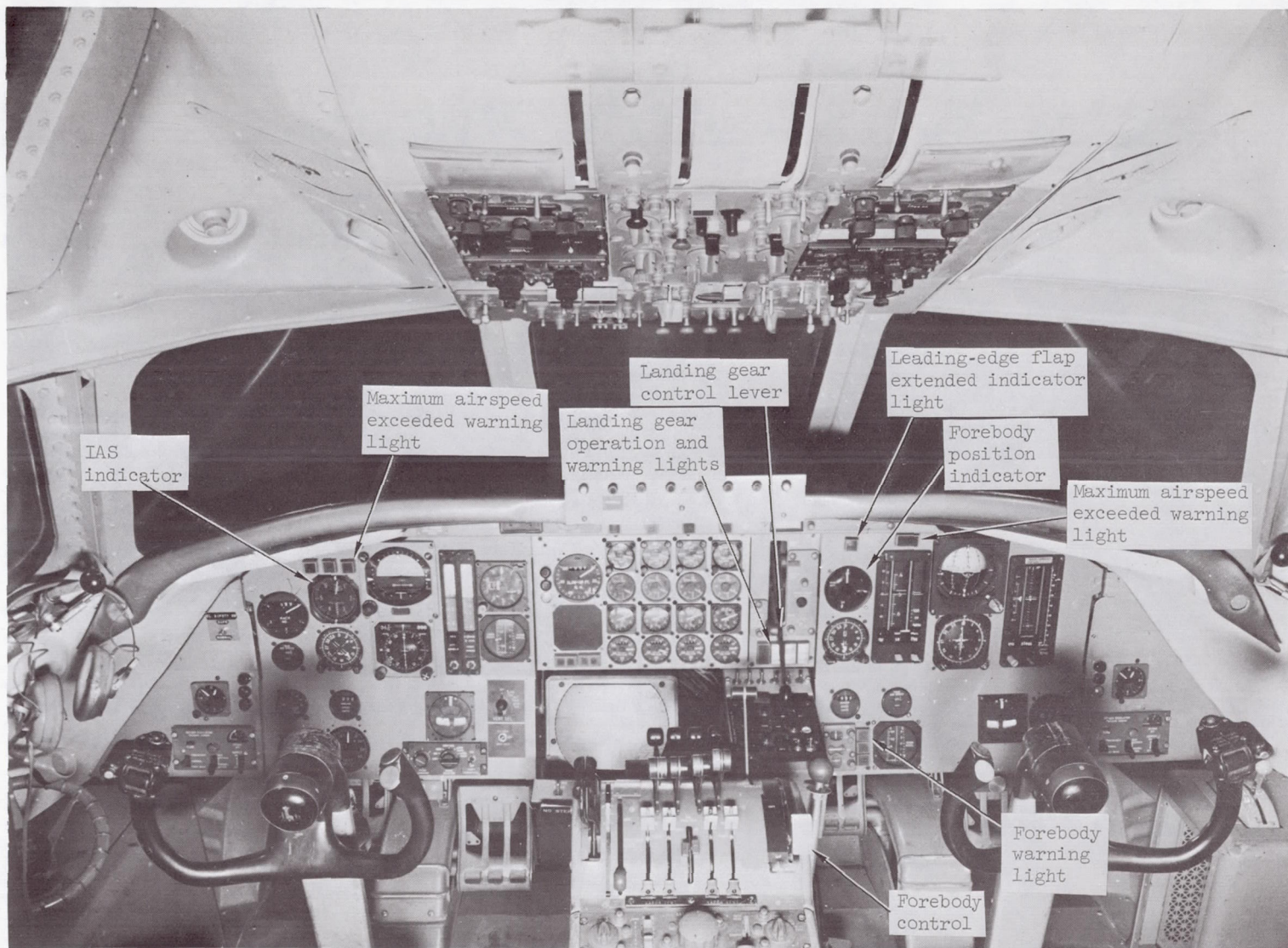


(a) SST configuration A.

L-68-4293.1

Figure 2.- Fixed-base SST simulator cockpit at Langley Research Center.





(b) SST configuration B.

L-66-6221.1

Figure 2.- Concluded.



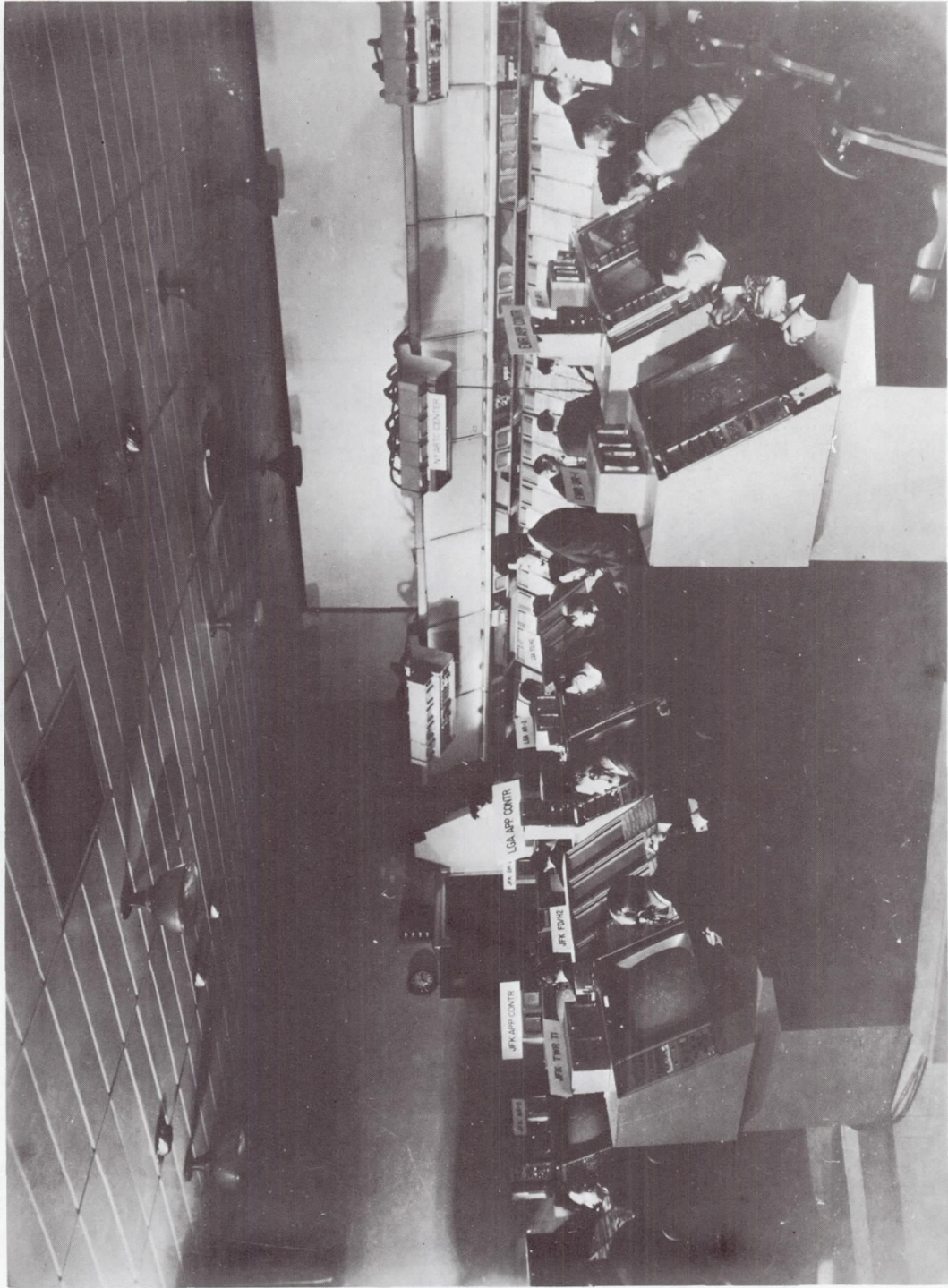


Figure 3.- Simulated ATC facility at NAFEC.

L-68-855



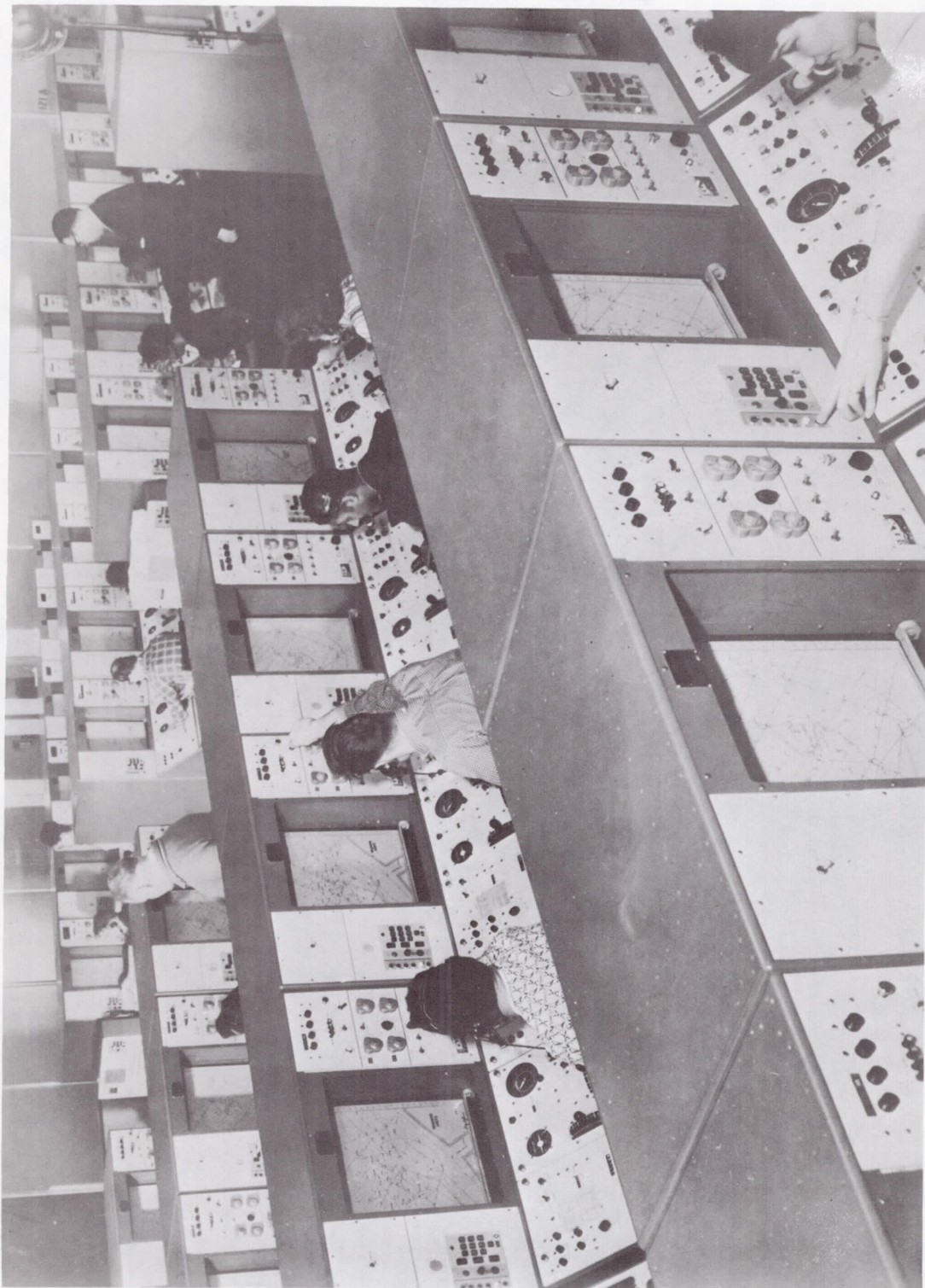
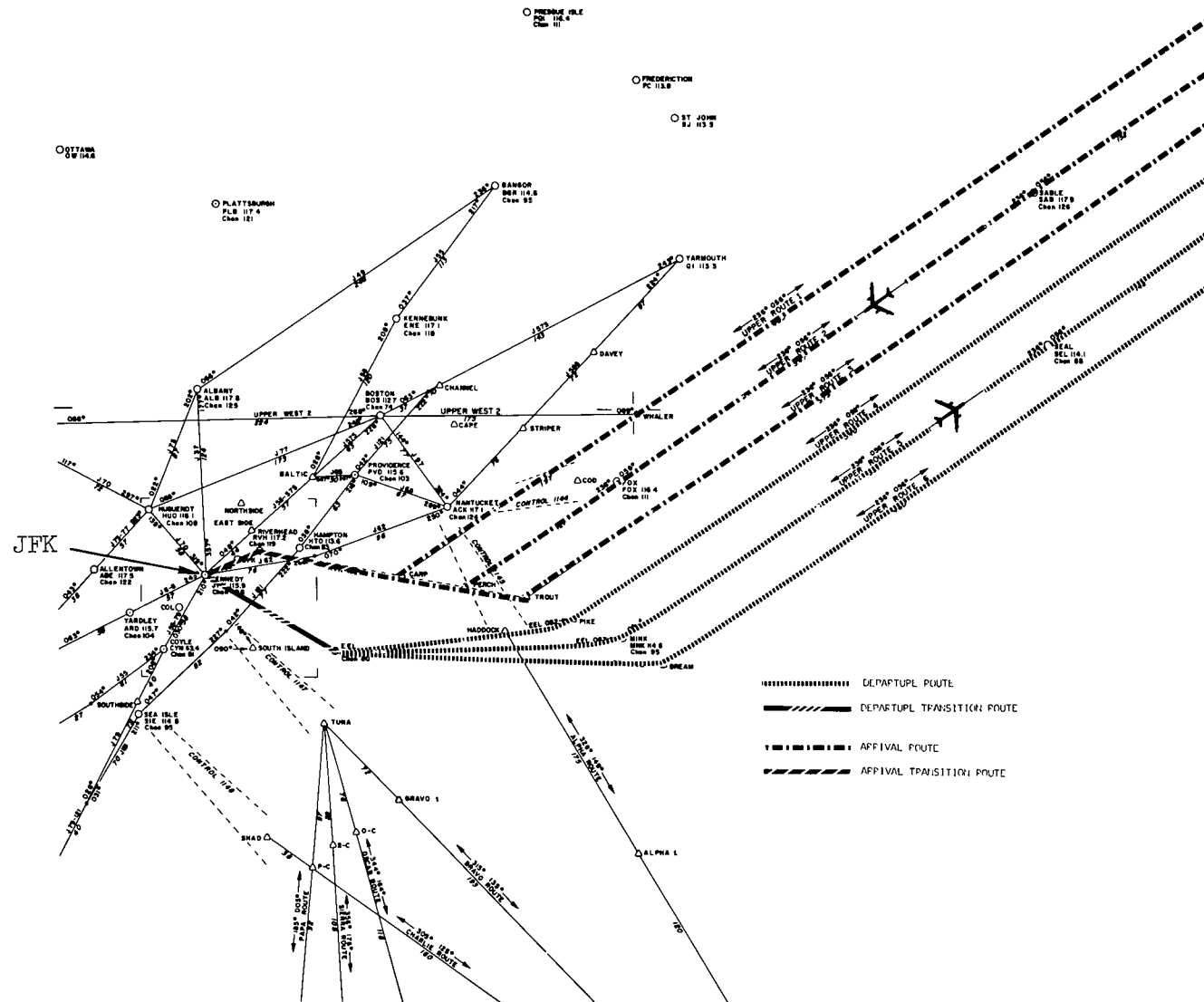


Figure 4.- Radar target generators at NAFEC.

L-68-856



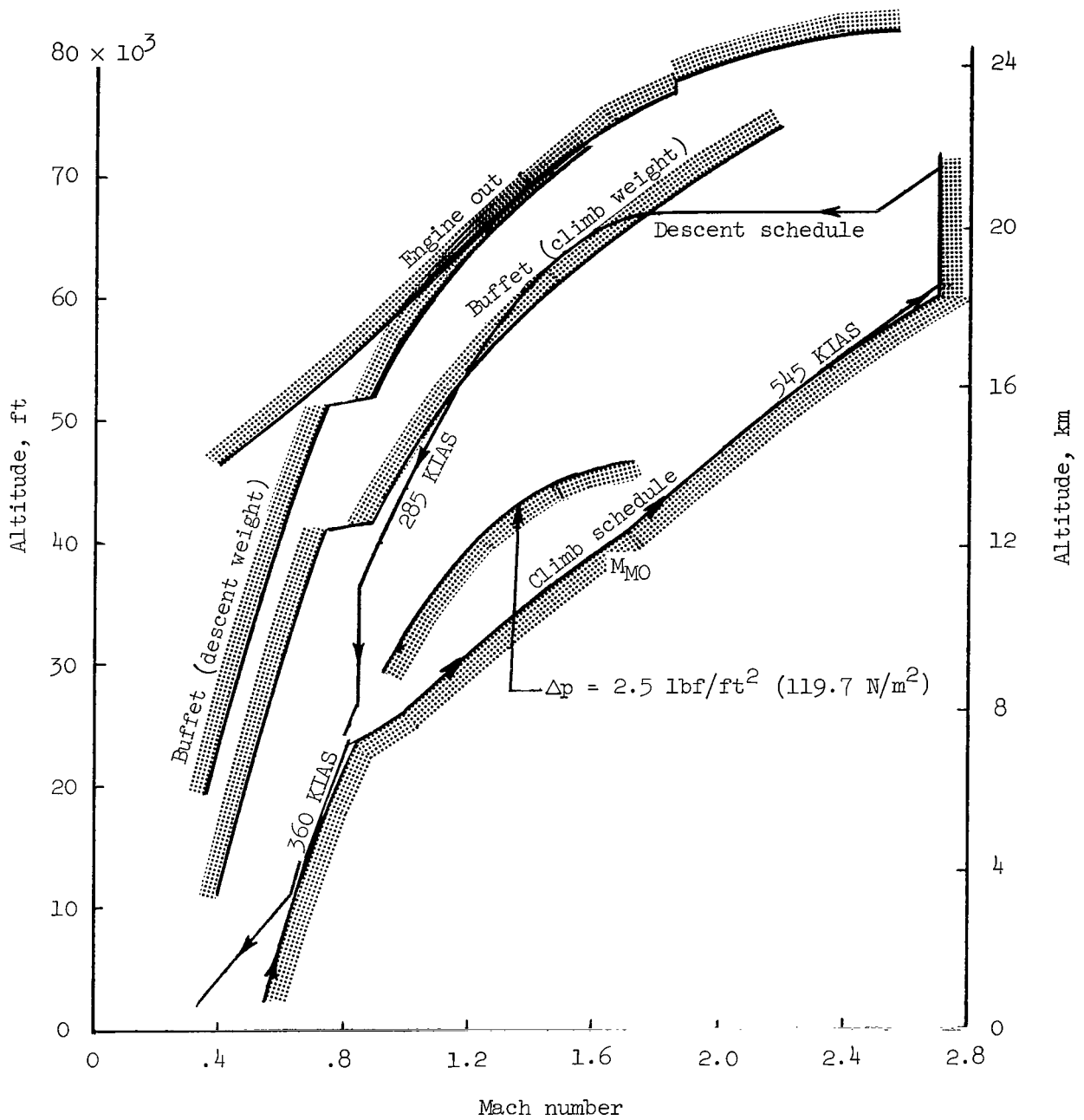
(a) JFK oceanic.

Figure 5.- Test areas and route structures.





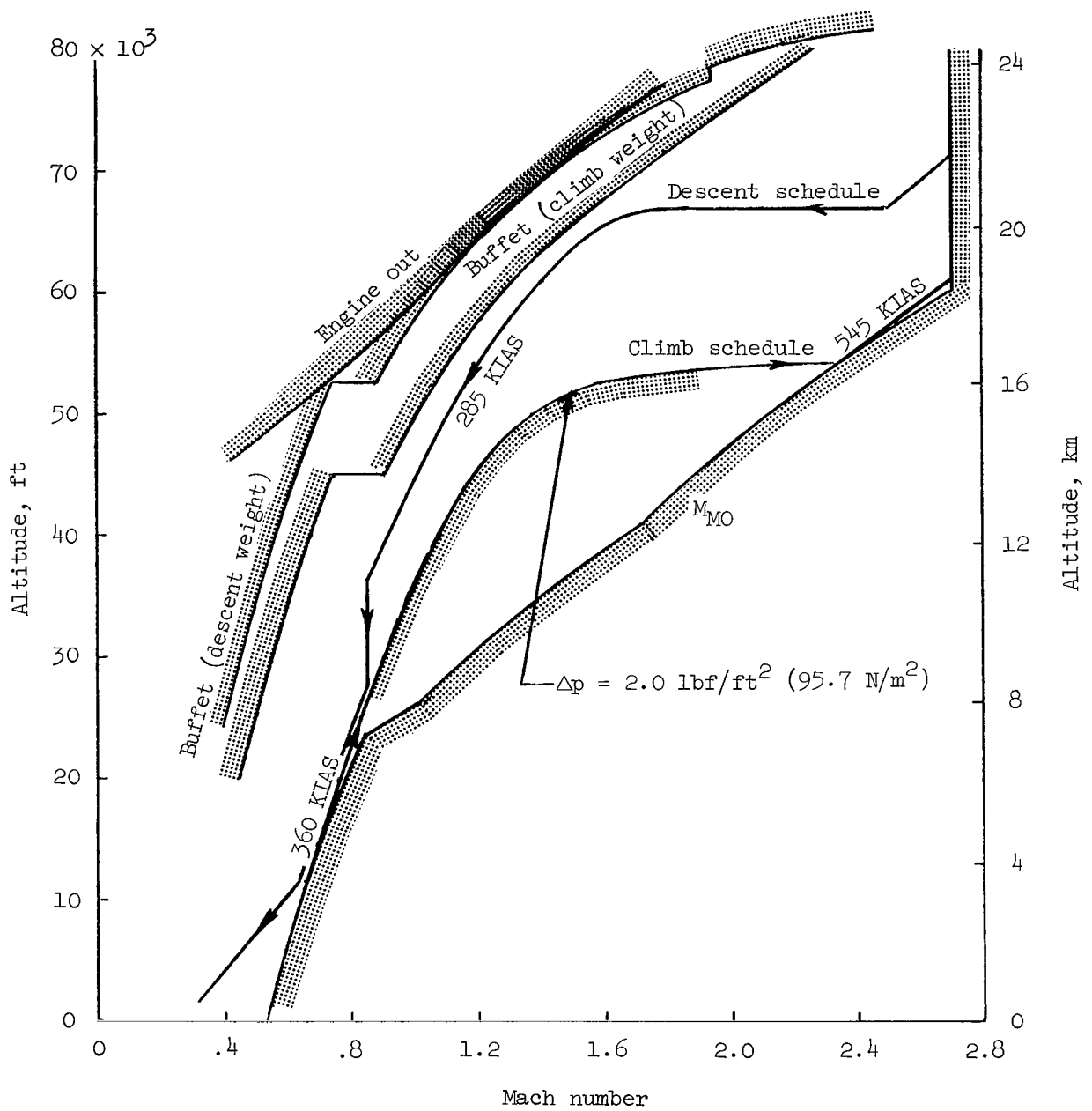




(a) Oceanic operations.

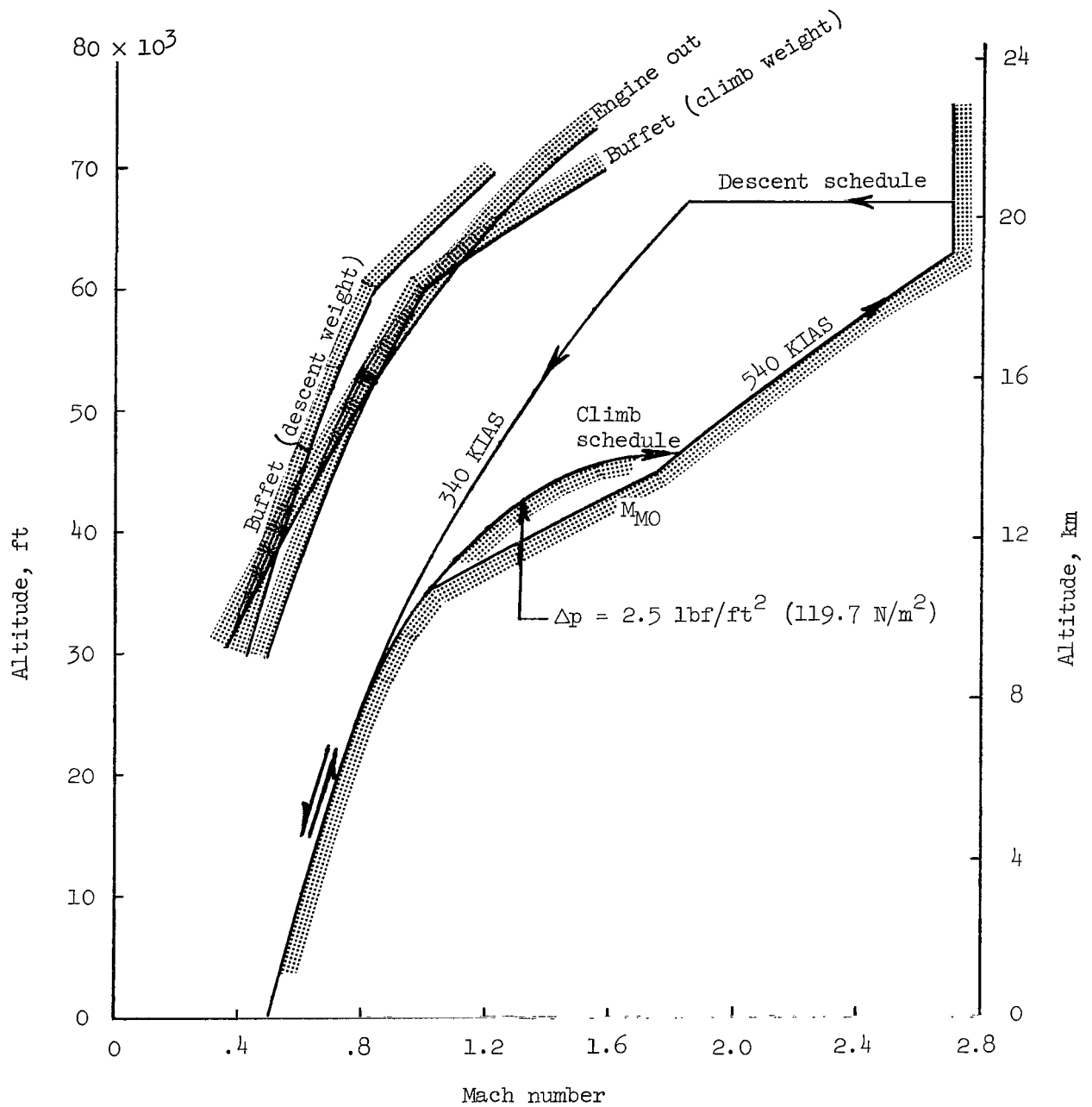
Figure 6.- Climb and descent schedules and flight limit boundaries. SST configuration A.





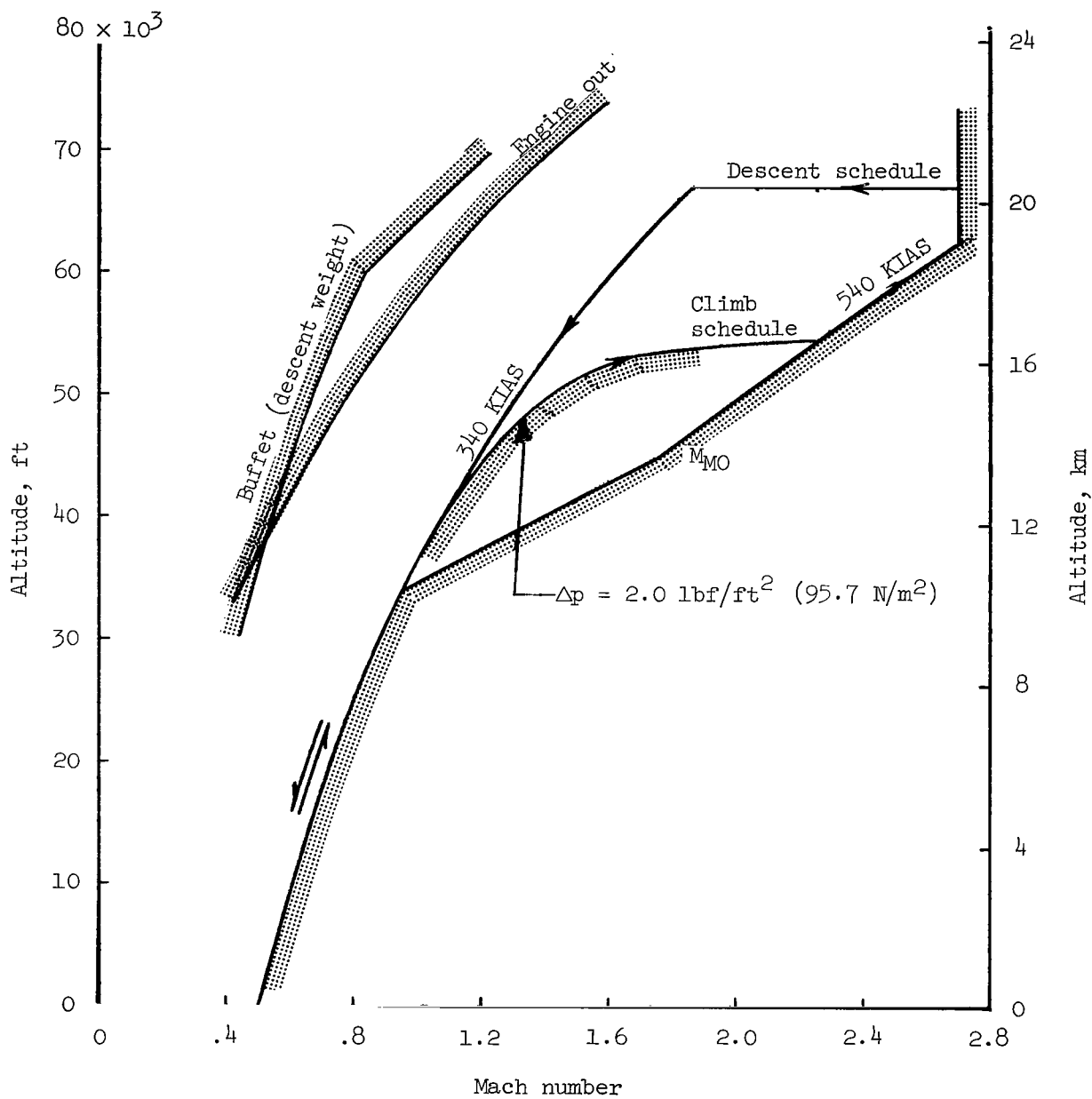
(b) Domestic operations.

Figure 6.- Concluded.



(a) Oceanic operations.

Figure 7.- Climb and descent schedules and flight limit boundaries. SST configuration B.



(b) Domestic operations.

Figure 7.- Concluded.

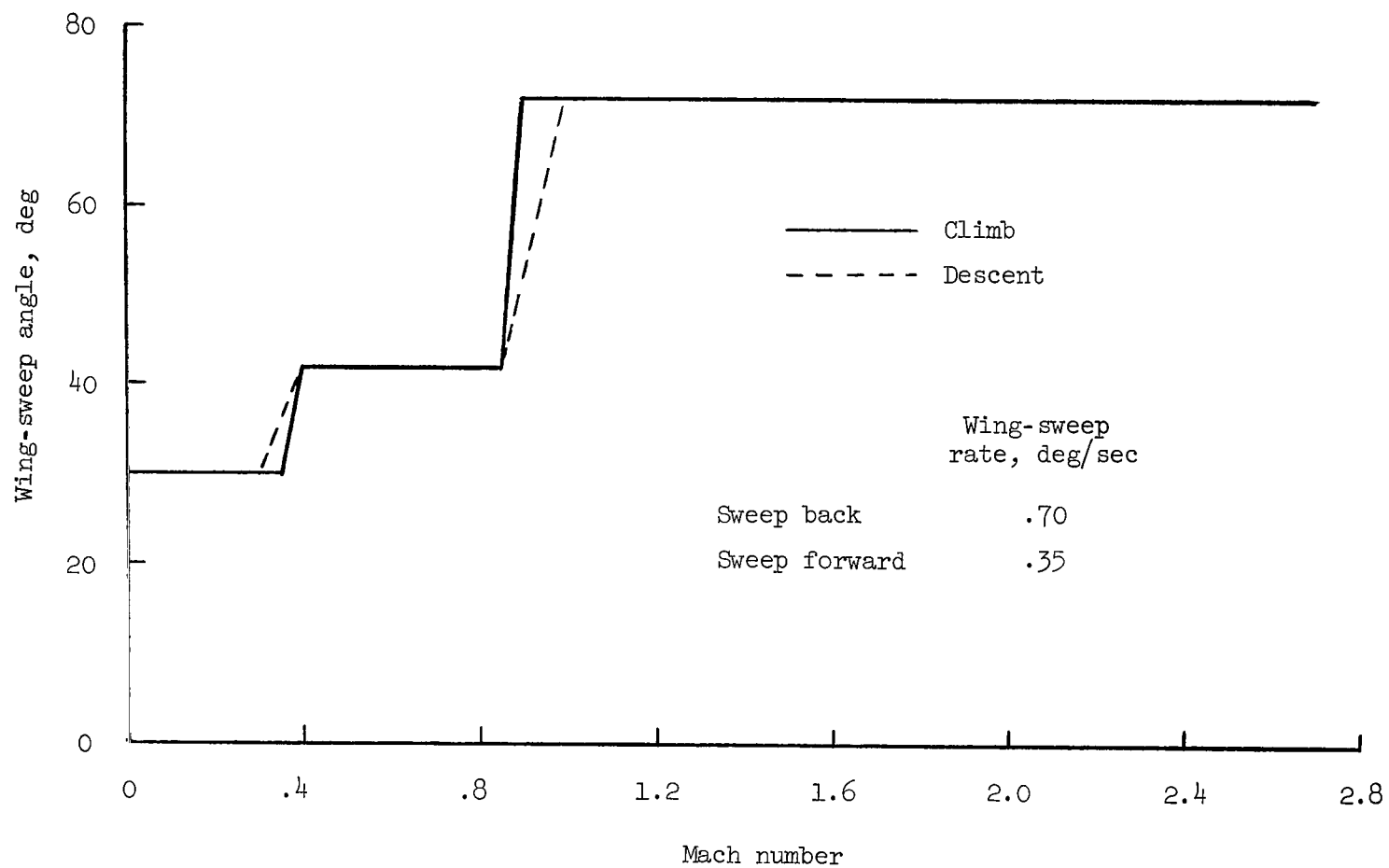
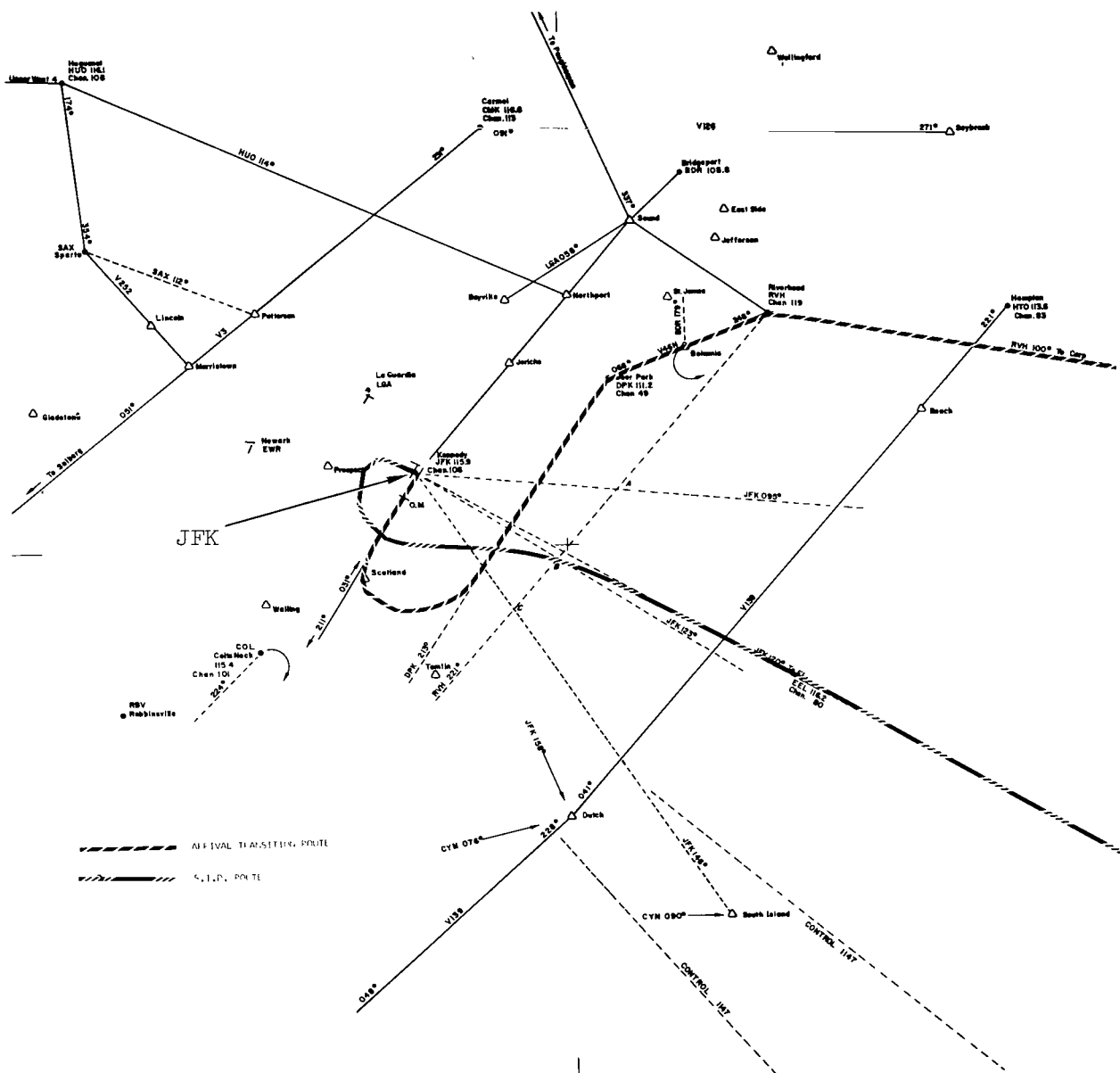
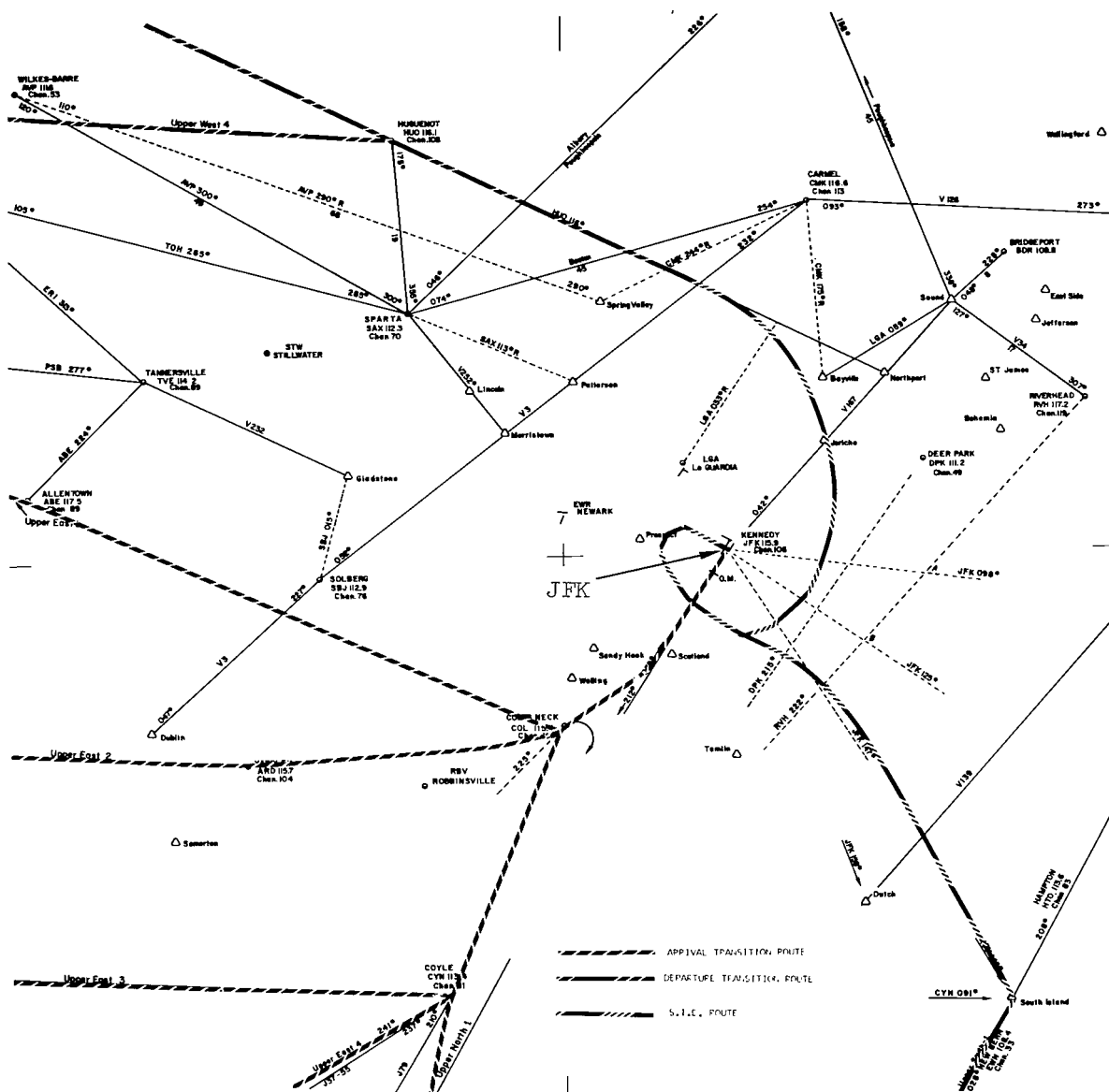


Figure 8.- Manual wing-sweep programs. SST configuration A.



(a) JFK oceanic operations.

Figure 9.- Standard instrument departure and terminal arrival routes. JFK and LAX areas.



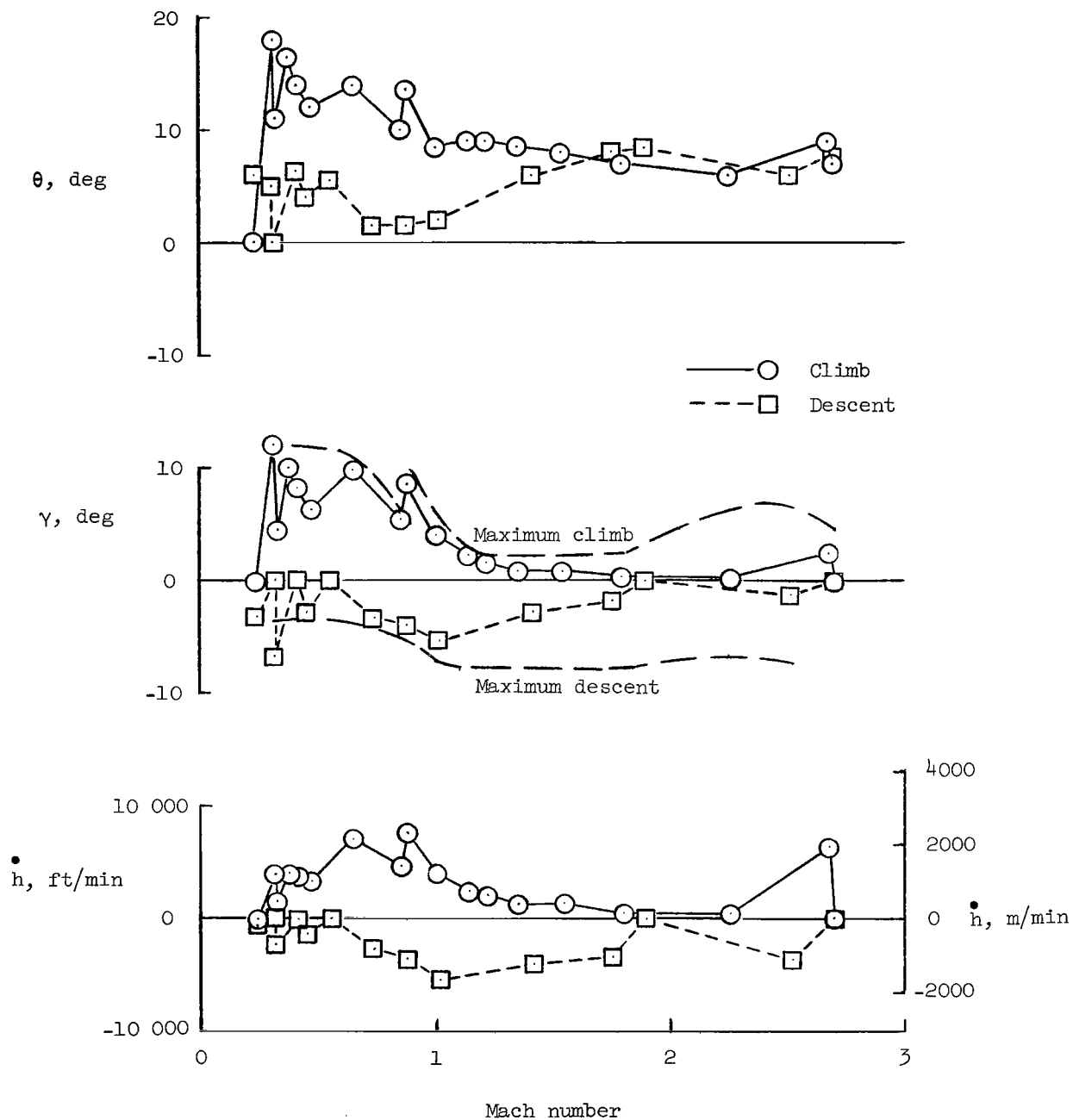
(b) JFK domestic operations.

Figure 9.- Continued.



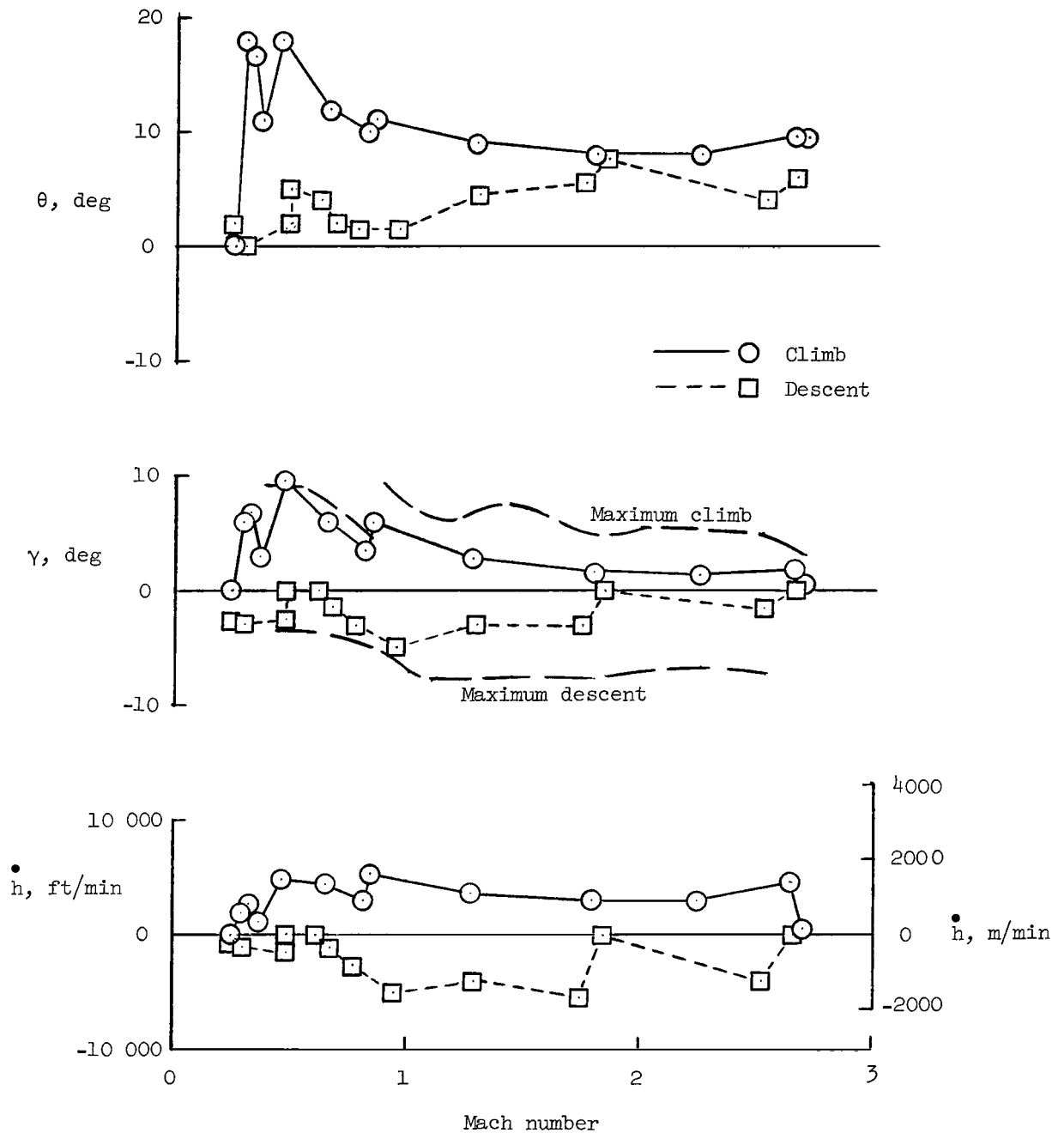






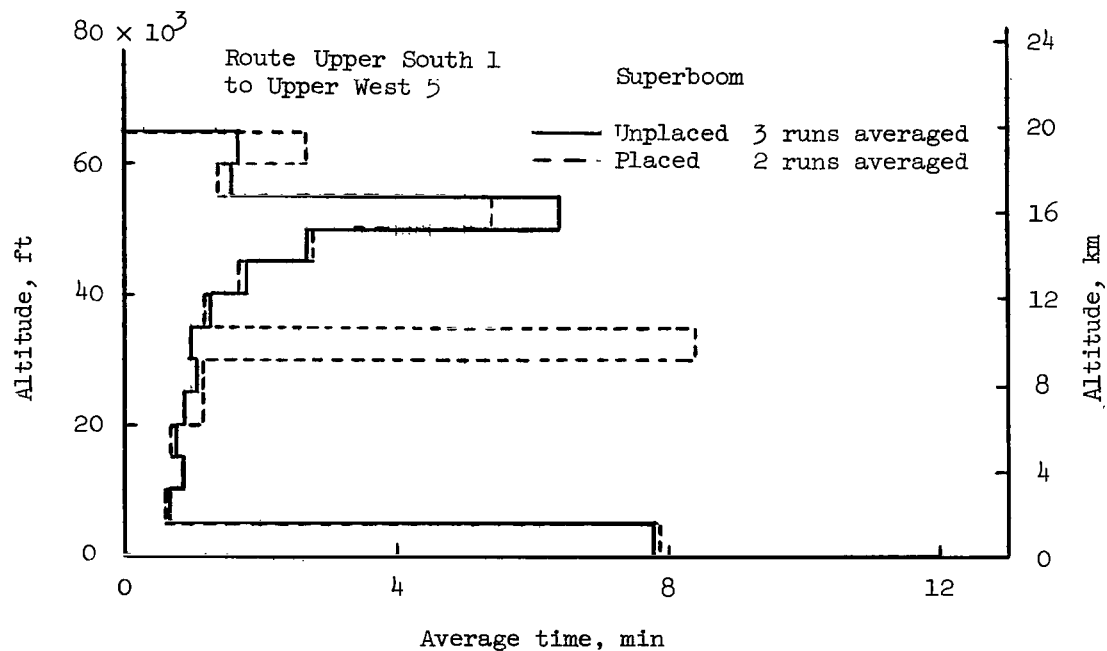
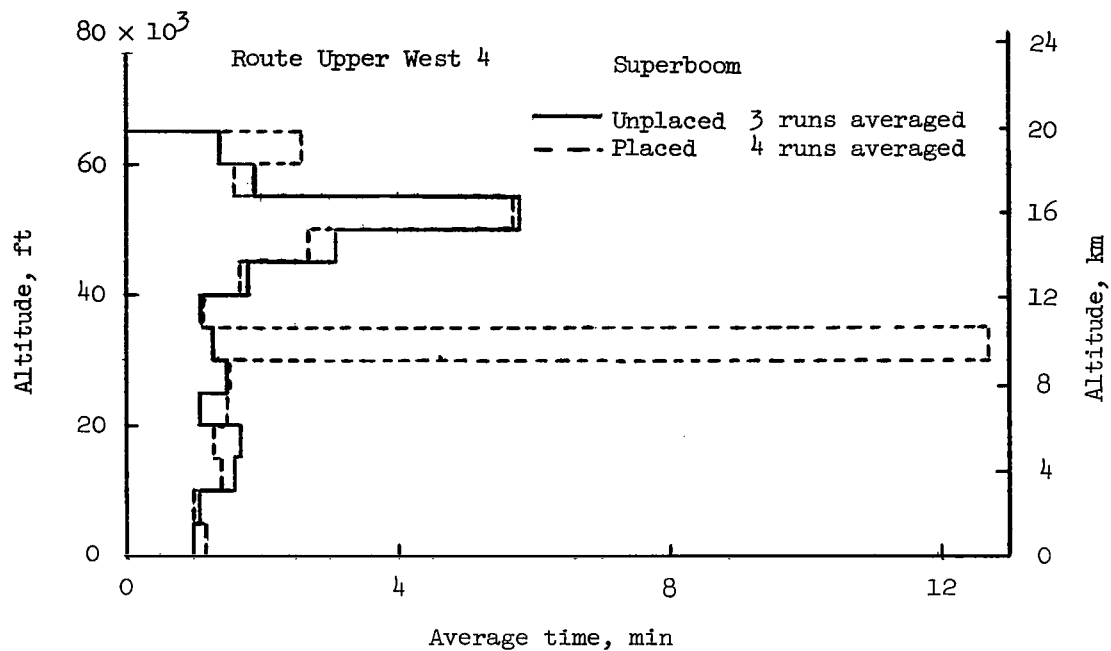
(a) Domestic operations.

Figure 10.- Typical variations of pitch attitude, flight-path angle, and vertical speeds with Mach number in climb and descent. Domestic and oceanic operations. SST configuration A.



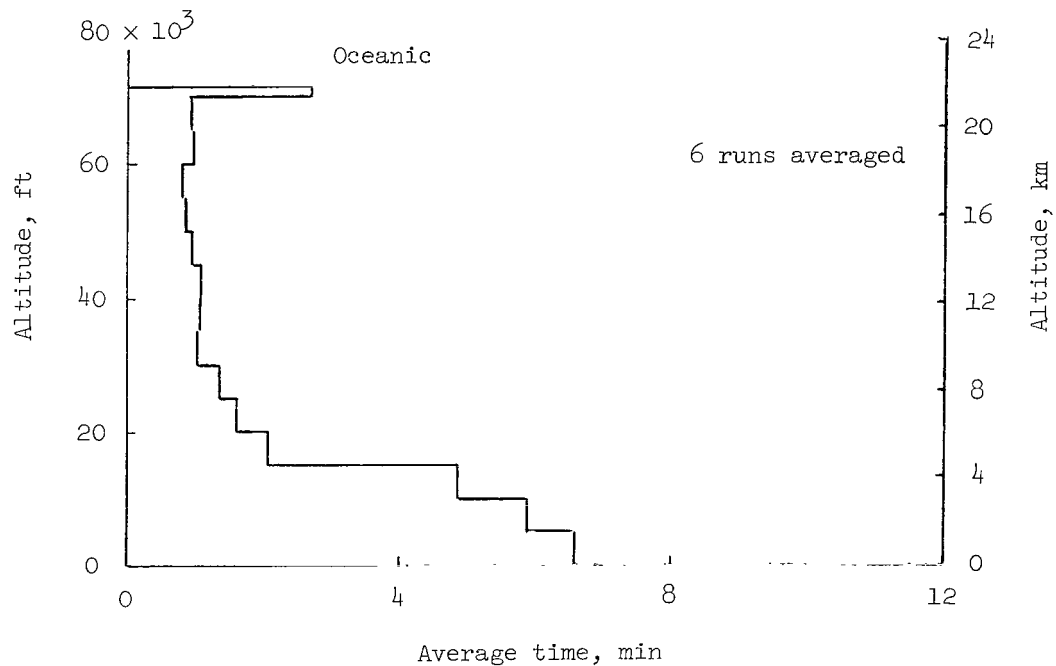
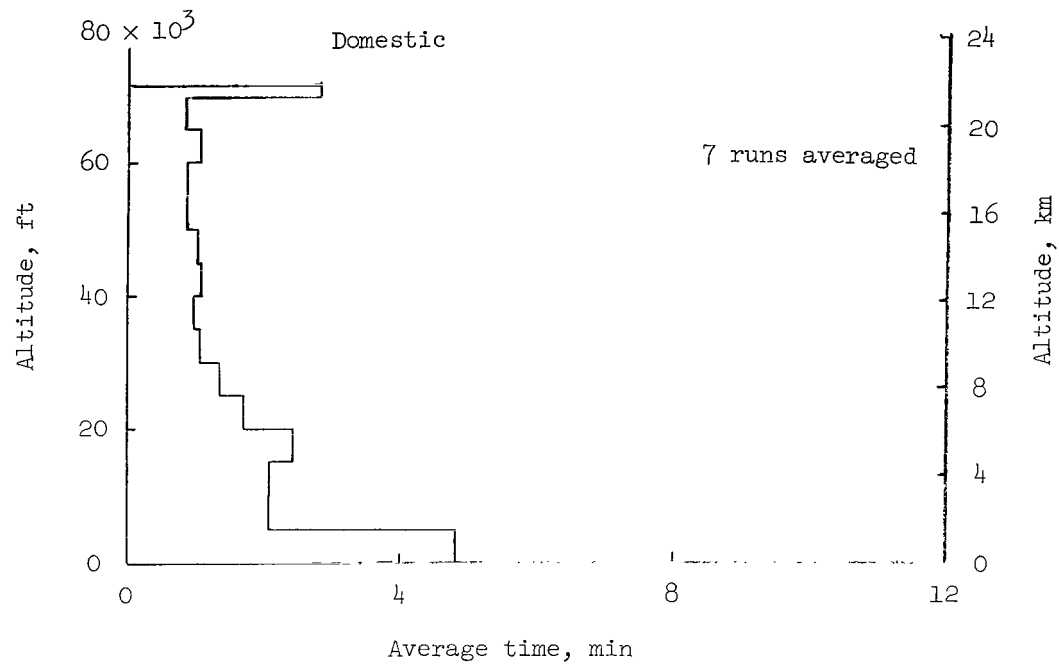
(b) Oceanic operations.

Figure 10.- Concluded.



(a) Departures.

Figure 11.- Histogram of average operating times at various altitudes for domestic arrival and departure operations at JFK.  
SST configuration B.



(b) Arrivals.

Figure 11.- Concluded.

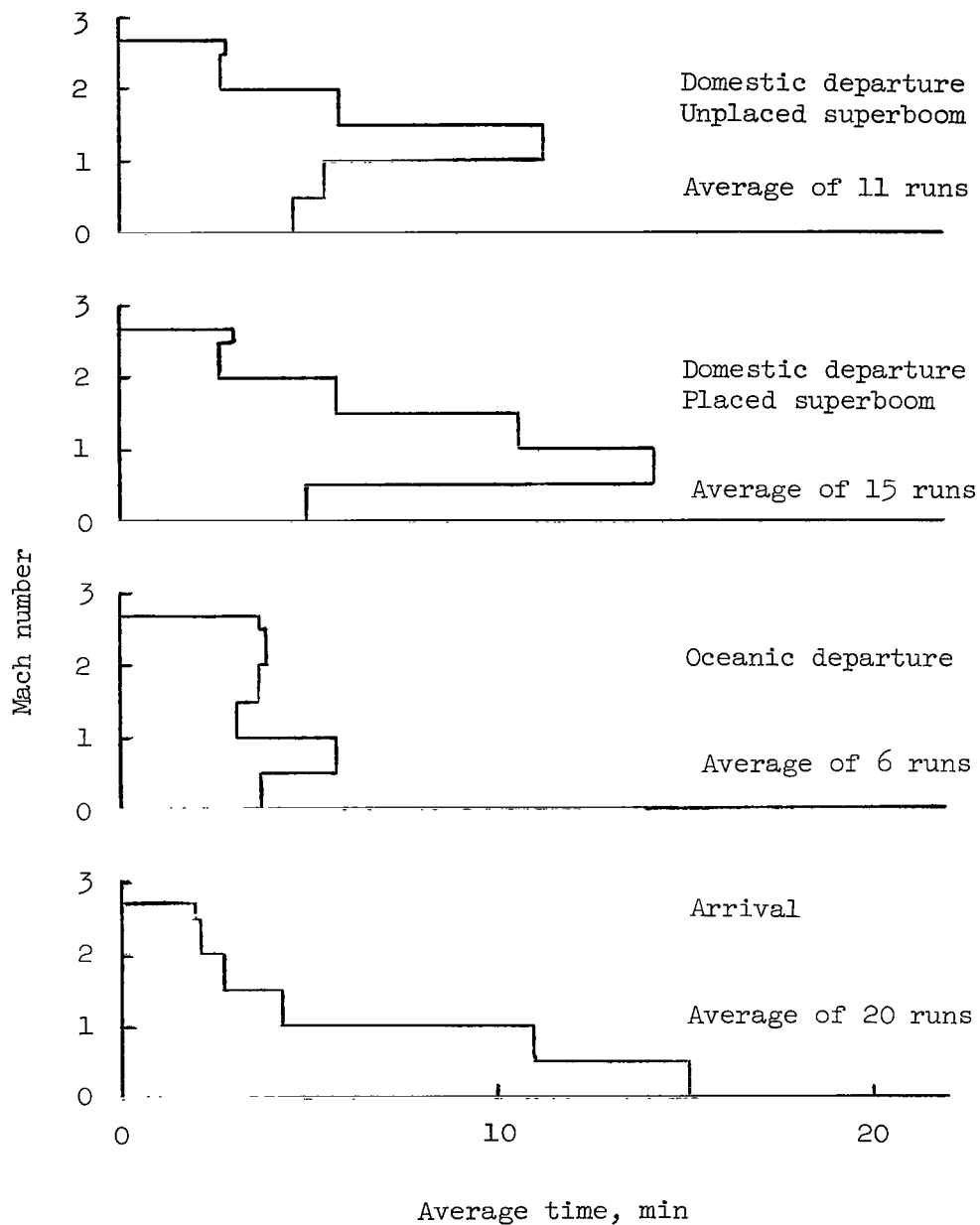
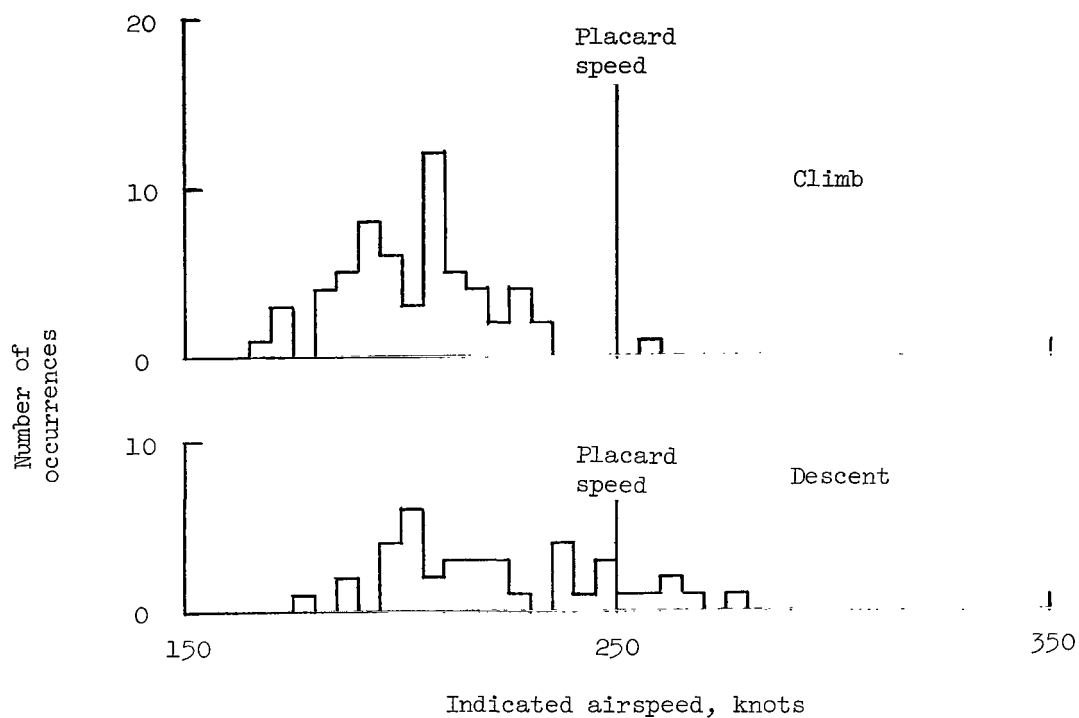
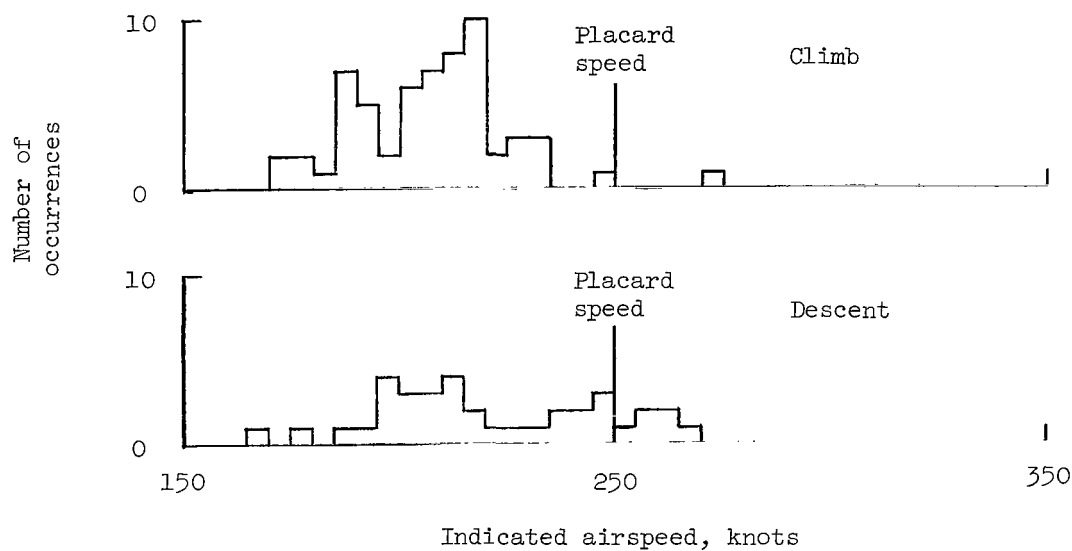


Figure 12.- Histograms of average operating times at various Mach numbers for domestic and oceanic departure and arrival operations at LAX. SST configuration A.

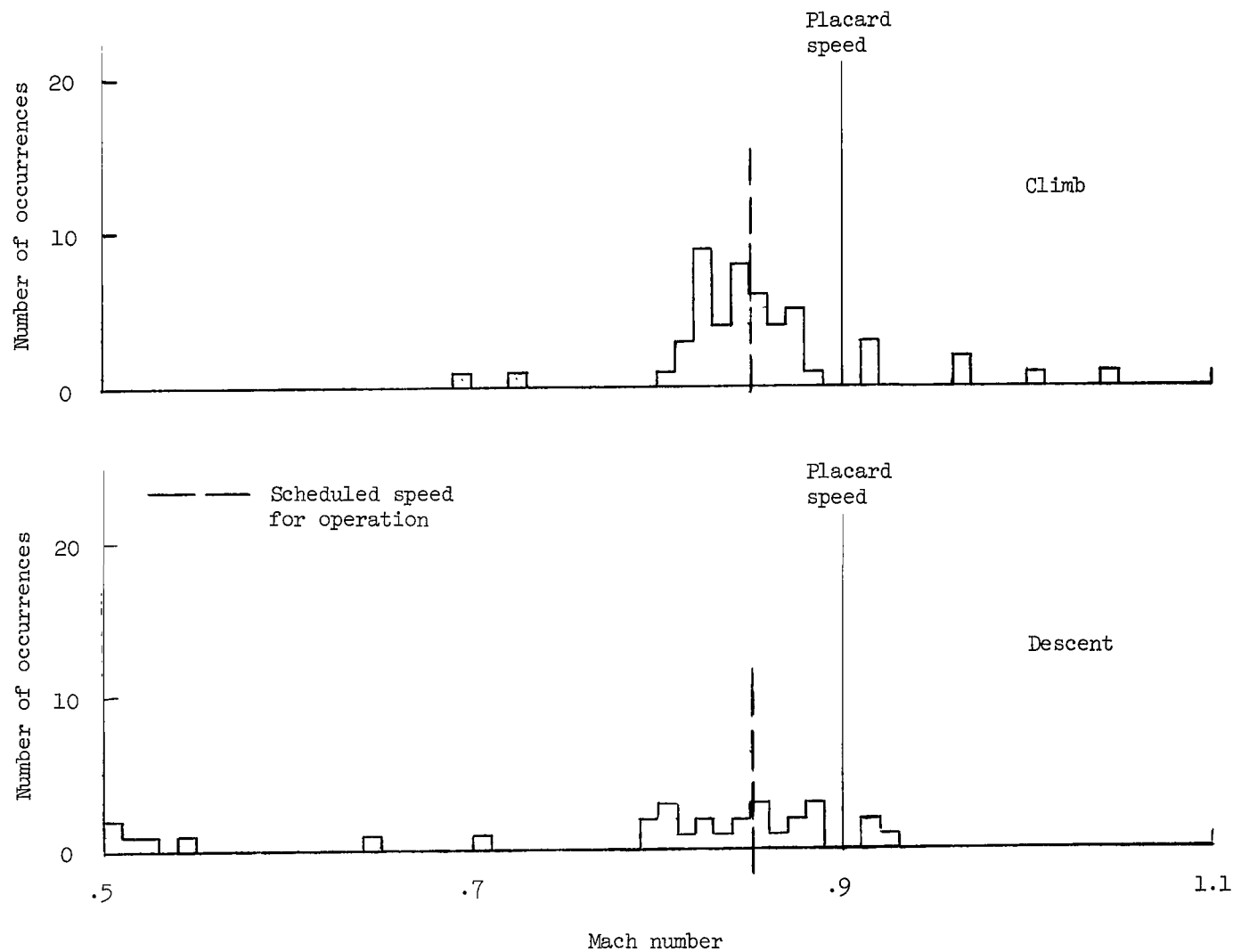


(a) Forebody deflected.



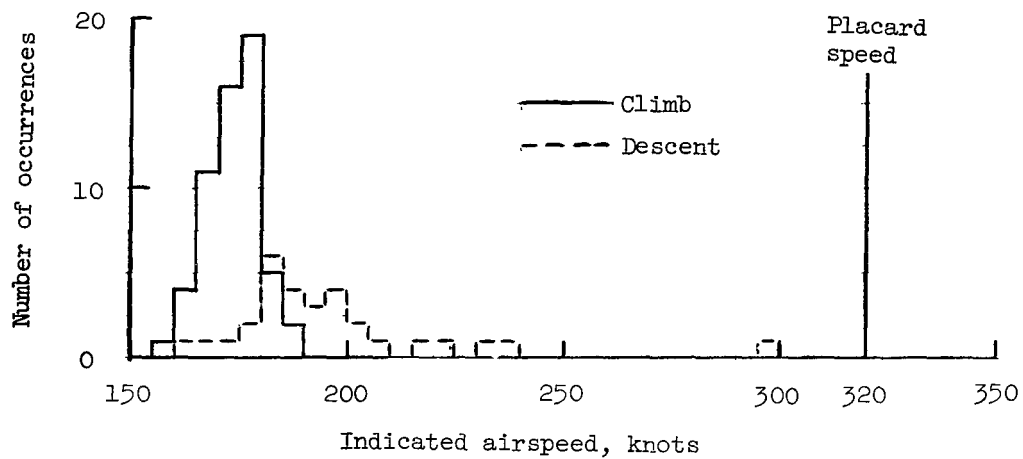
(b) Landing gear extended or actuating.

Figure 13.- Histograms of maximum recorded airspeed with forebody deflected and with landing gear extended or actuating. Climb and descent operations; SST configuration B.

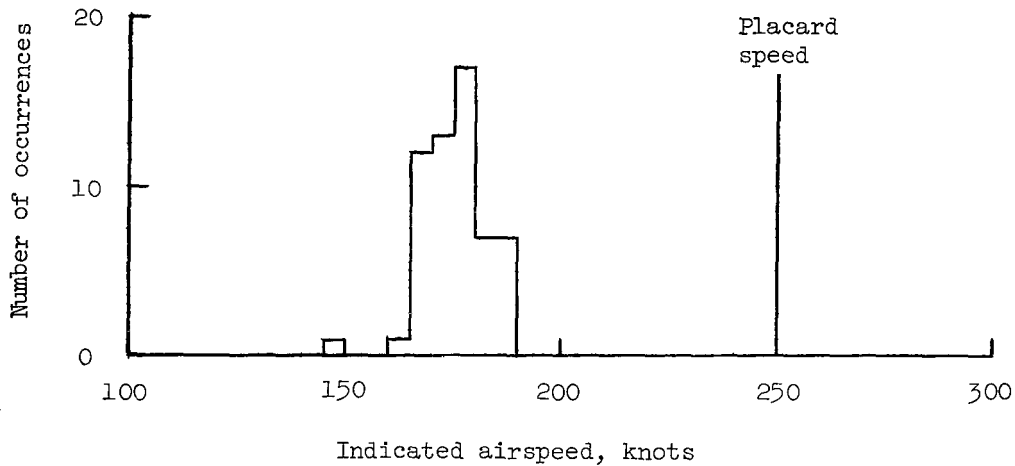


(a) Forebody deflected.

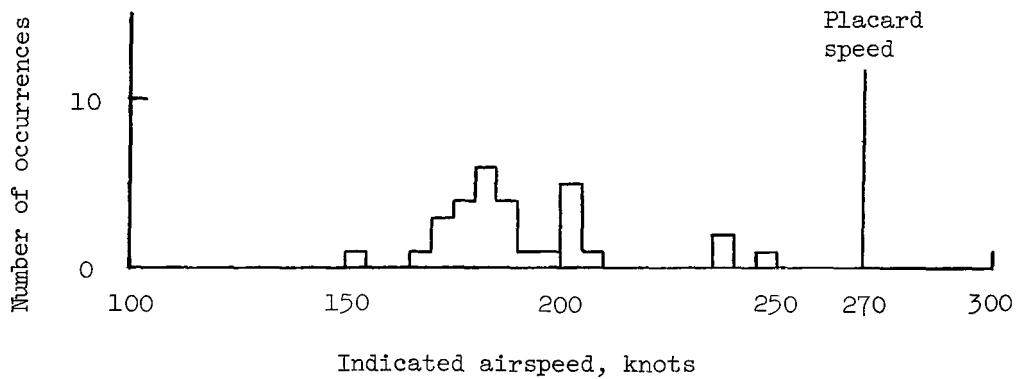
Figure 14.- Histograms of maximum recorded speed with forebody deflected; landing gear extended, retracting, and extending; and flaps deflected configurations. Climb and descent operations; SST configuration A.



(b) Landing gear extended.



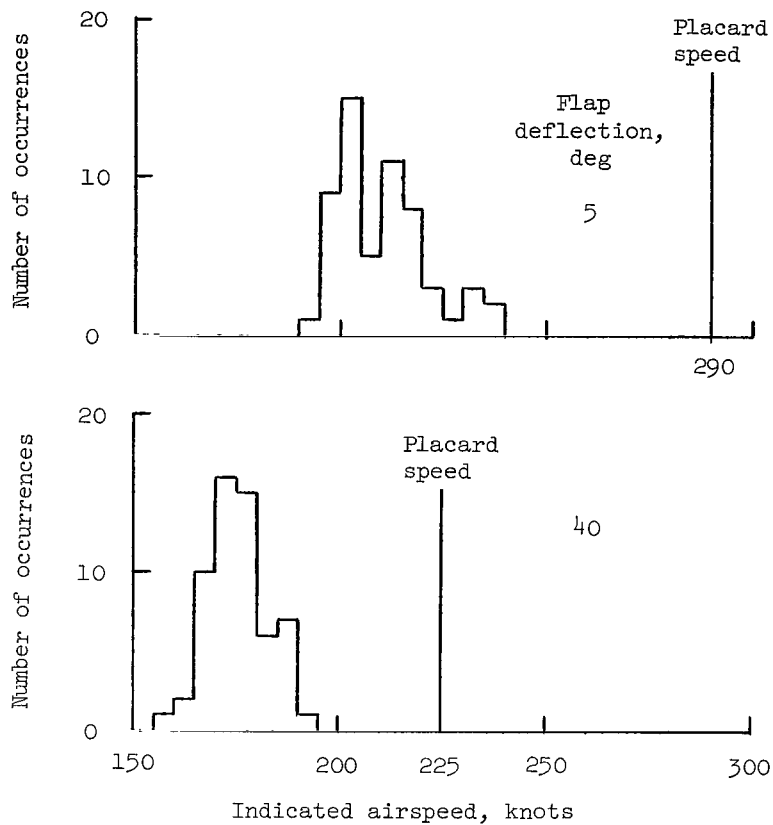
(c) Landing gear retracting.



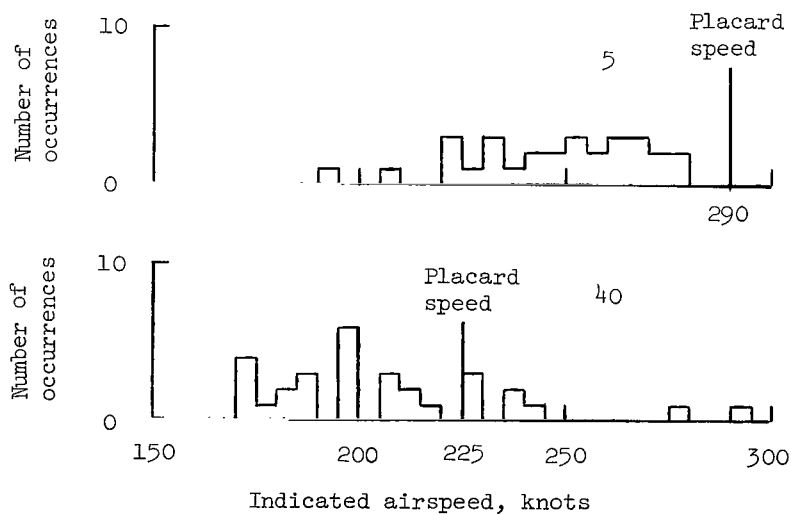
(d) Landing gear extending.

Figure 14.- Continued.



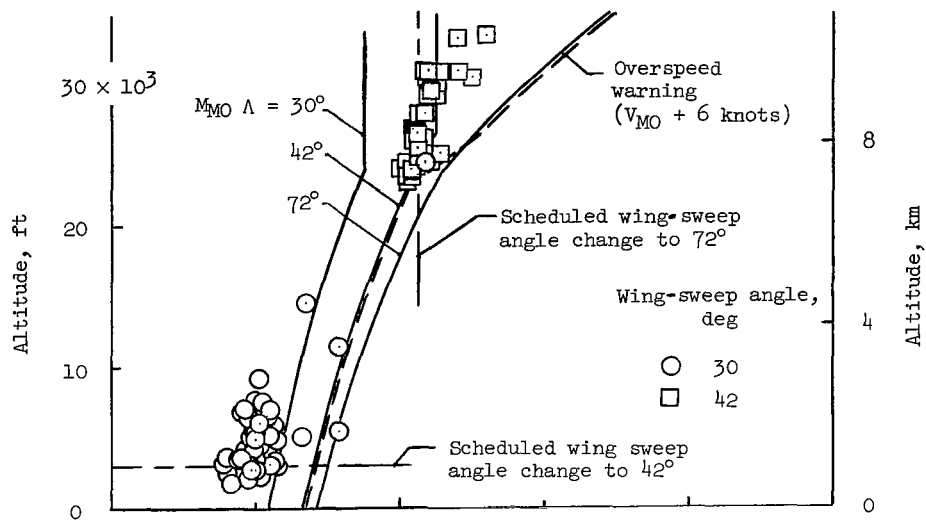


(e) Flaps deflected; climb operations.

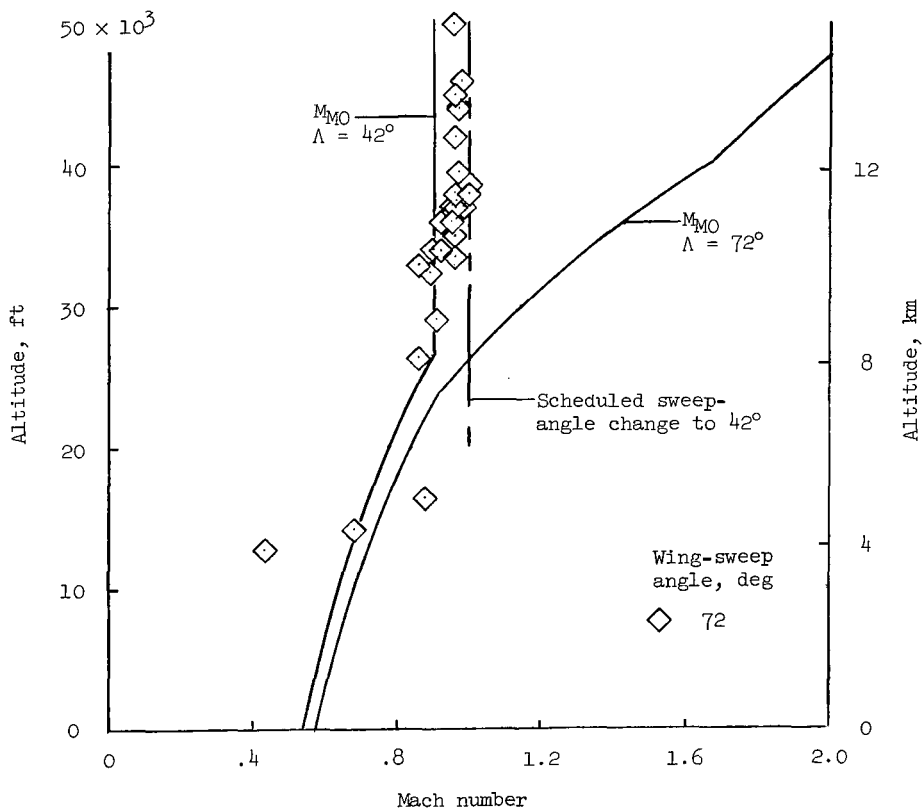


(f) Flaps deflected; descent operations.

Figure 14.- Concluded.

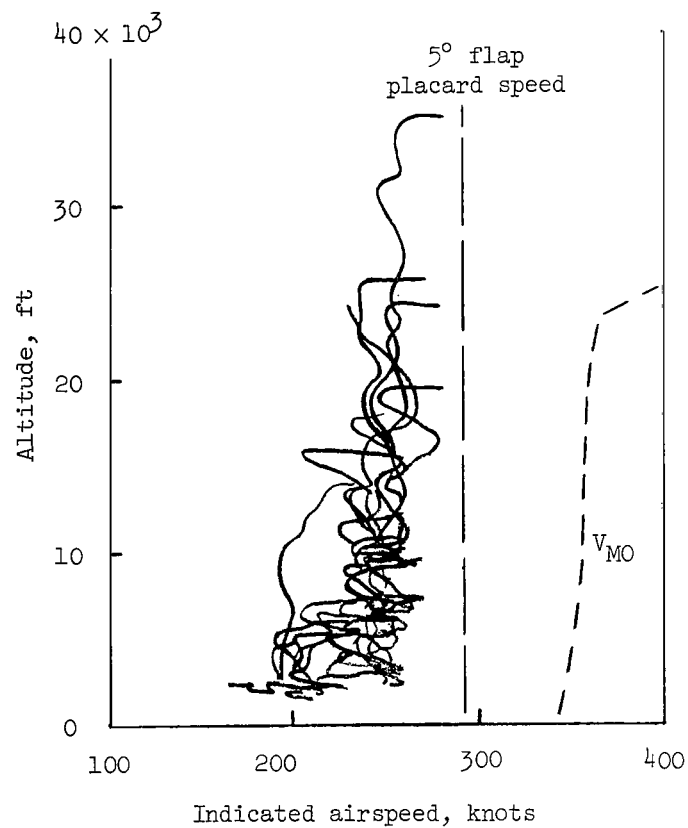


(a) Clim.

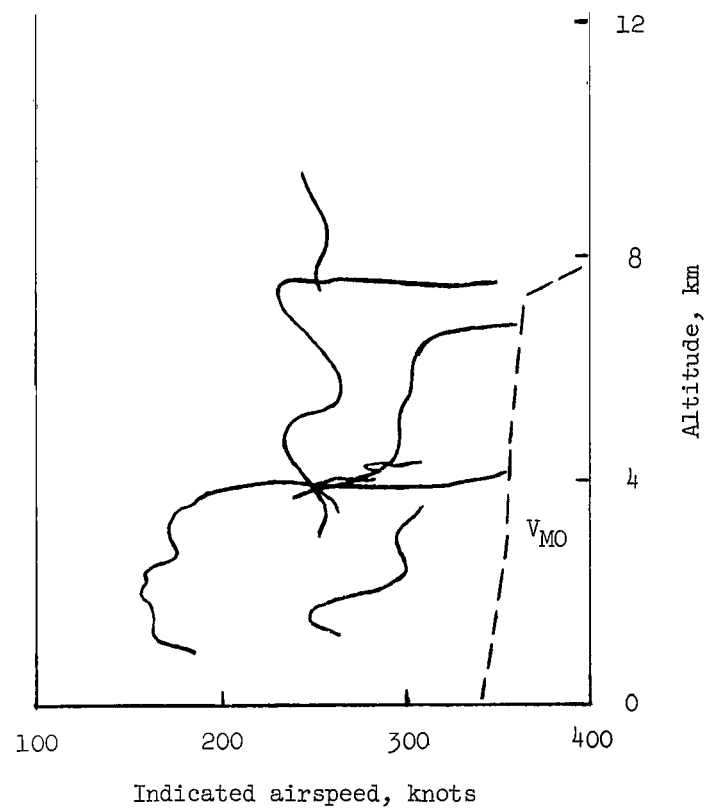


(b) Descent.

Figure 15.- Maximum recorded speeds in climb with  $\Lambda = 30^\circ$  and  $42^\circ$  and minimum operating speeds in descent with  $\Lambda = 72^\circ$ . Scheduled altitudes and speeds for  $\Lambda$  changes and  $M_{MO}$  boundaries shown; SST configuration A.



(a) 50/50 flap deflection.



(b) Spoilers extended.

Figure 16.- Altitude-speed histories of flap and spoiler operations in 27 descents. SST configuration A.

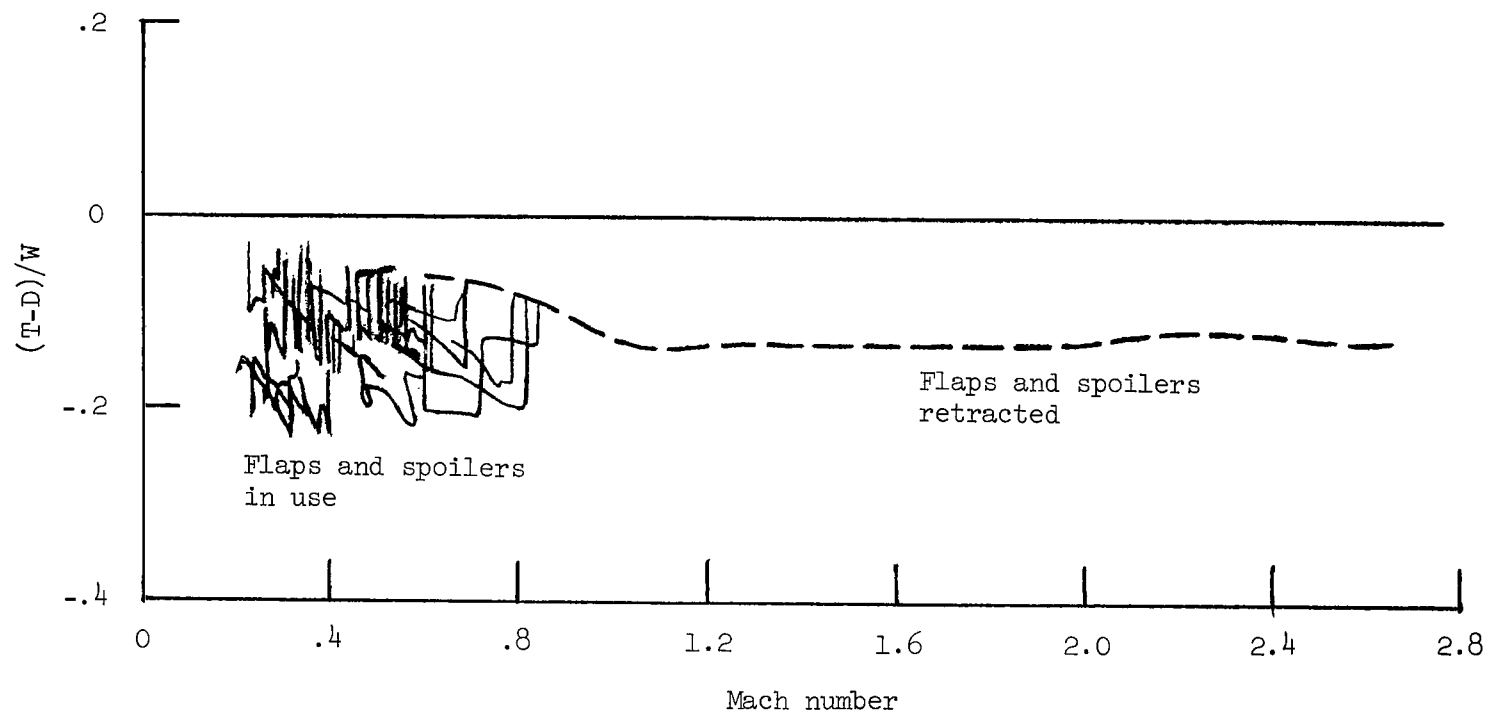
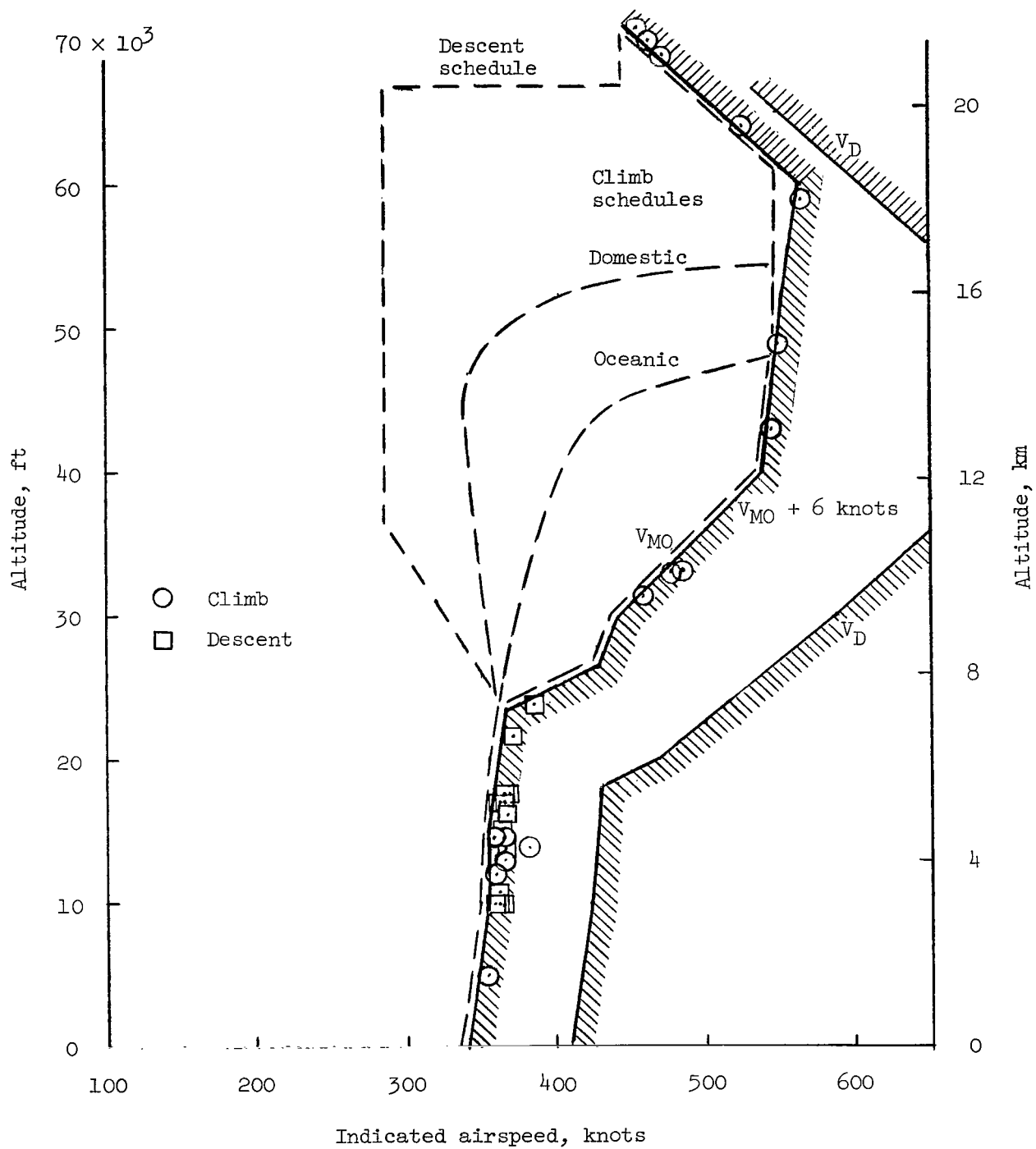
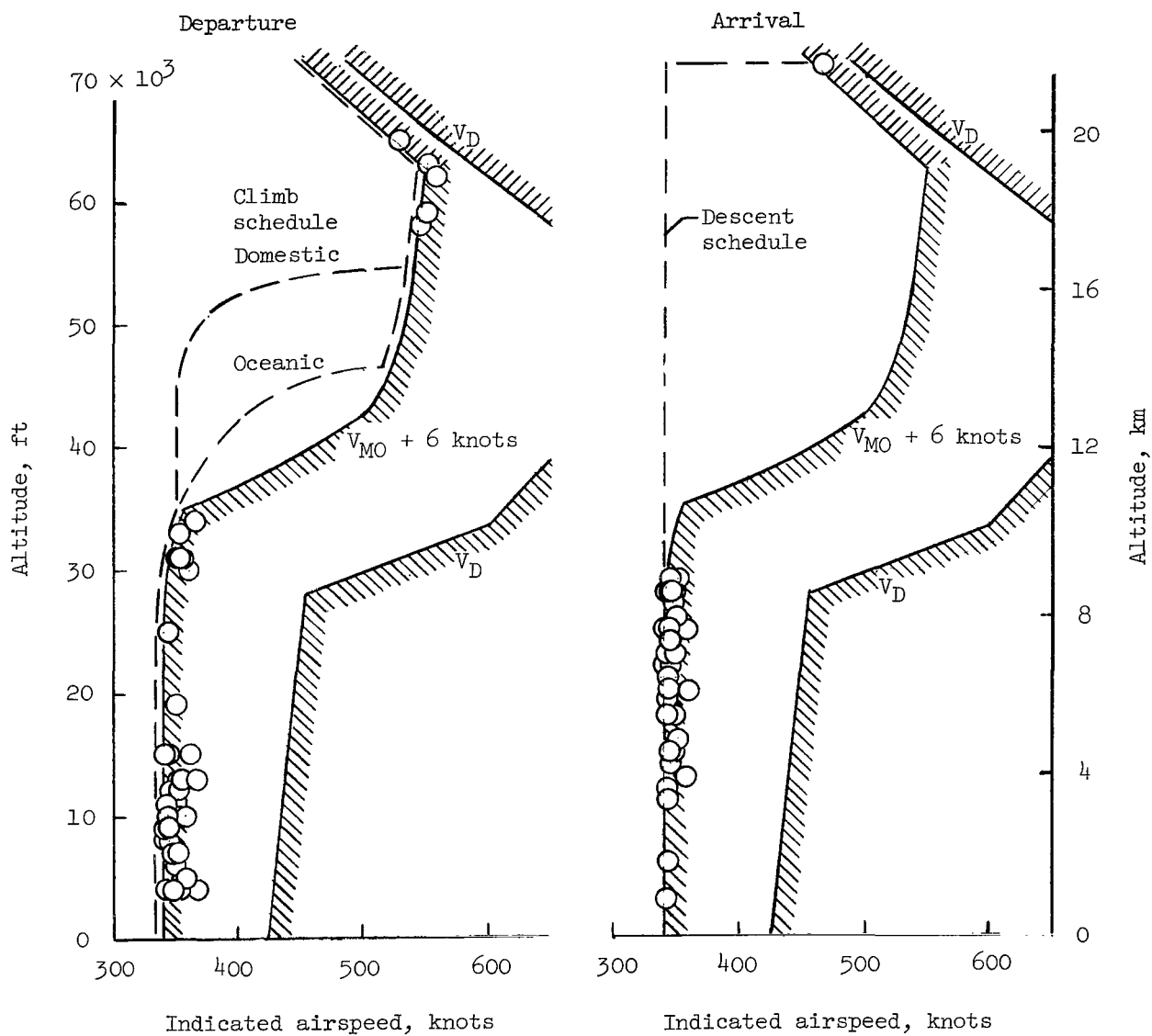


Figure 17.- Variation of  $(T - D)/W$  with Mach number in descents. Flight idle power; SST configuration A.



(a) SST configuration A. 10 arrivals; 12 departures.

Figure 18.- Overspeed events during climb and descent in both oceanic and domestic departure and arrival operations.



(b) SST configuration B. 55 departures; 38 arrivals.

Figure 18.- Concluded.

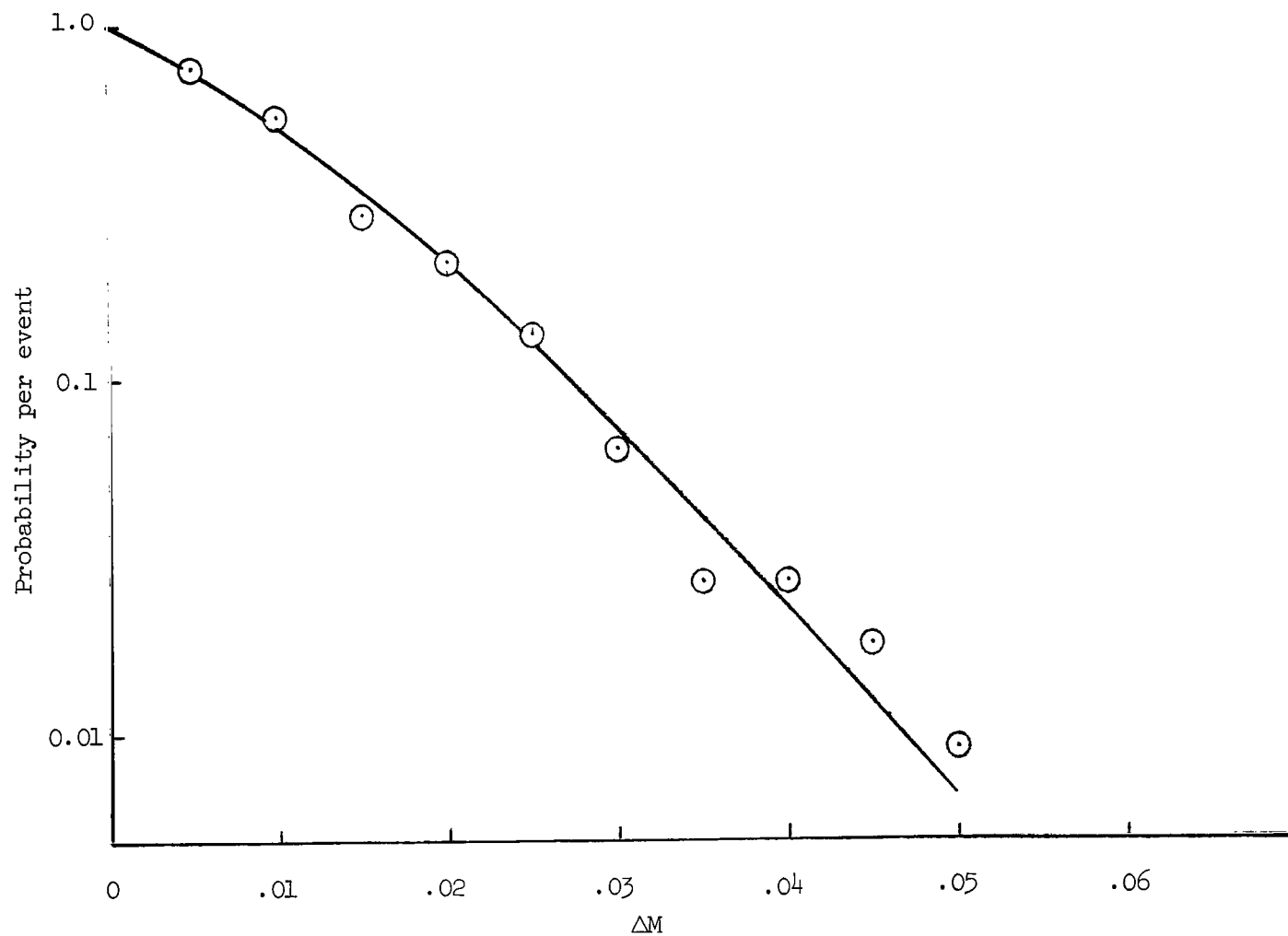
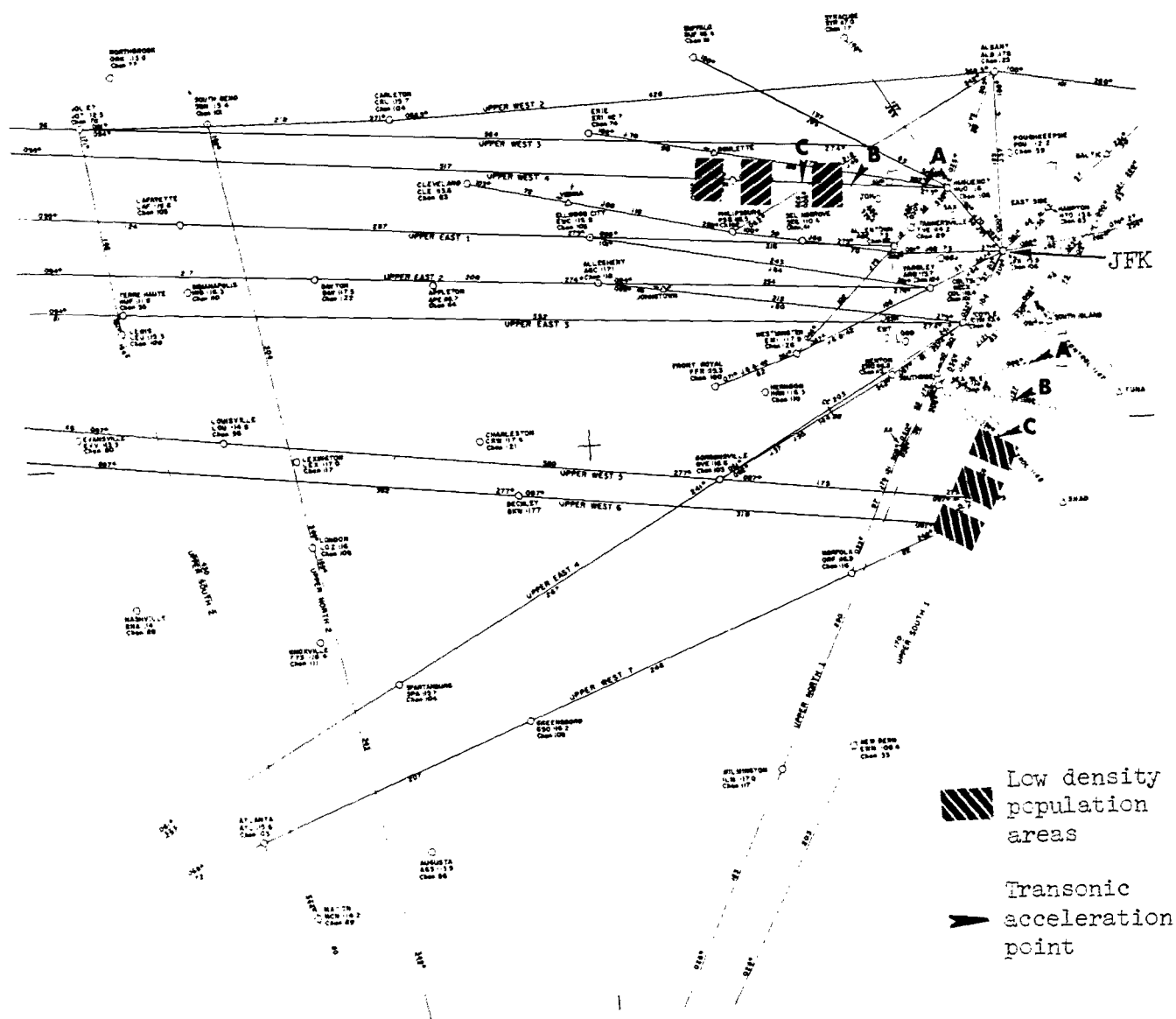


Figure 19.- Probability of equaling or exceeding  $M_{M0} = 2.7$  in cruise flight by Mach number increments  $\Delta M$ . SST configuration B; calm air standard atmospheric conditions.



(a) JFK area.

Figure 20.- Location of low-density population areas and transonic acceleration initiation points used in superboom placement operations. JFK and LAX areas.



